Cerebral Cortex September 2008;18:2141–2157
doi:10.1093/cercor/bhm241
Advance Access publication January 31, 2008

Probabilistic Maps, Morphometry, and Variability of Cytoarchitectonic Areas in the Human Superior Parietal Cortex

Filip Scheperjans[1,2], Simon B. Eickhoff[1], Lars Hömke[1], Hartmut Mohlberg[1], Klaudia Hermann[1,2], Katrin Amunts[1,3] and Karl Zilles[1,2]

[1]Institute of Medicine, Research Center Jülich, D-52425 Jülich, Germany, [2]C. & O. Vogt Institute for Brain Research, University of Düsseldorf, D-40001 Düsseldorf, Germany and [3]Department of Psychiatry and Psychotherapy, Aachen University Hospital, D-52074 Aachen, Germany

Recently, 8 areas (5Ci, 5M, 5L, 7PC, 7A, 7P, 7M, hIP3) in the human superior parietal cortex (SPC) were delineated in 10 postmortem brains using observer-independent cytoarchitectonic analysis. Here we present 3D probabilistic maps of these areas, quantifying the interindividual overlap for each voxel in stereotaxic reference space, and a maximum probability map, providing a contiguous parcellation. For all areas, we determined probabilities of mutual borders, calculated stereotaxic centers of gravity, and estimated volumes. A basic pattern of areas and borders was observed, which showed, however, intersubject variations and a significant interhemispheric asymmetry (7P, 7M) that may be functionally relevant. There was a trend toward higher intersubject anatomical variability in lateral compared with medial areas. For several areas (5M, 7PC, 7A, 7P), variability was significantly higher in the left hemisphere and/or in men, whereas for areas 5Ci and 5M there was a hemisphere-by-gender interaction. Differences in anatomical variability could bias group analyses in functional imaging studies by reducing sensitivity for activations of entities with high variability. The probabilistic maps provide an objective anatomical reference and account for the structural variability of the human brain. Integrated into functional imaging experiments, they can improve structure–function investigations of the human SPC.

Keywords: area 5, area 7, brain mapping, intraparietal sulcus (IPS), precuneus, superior parietal lobule (SPL)

Introduction

Macroanatomically, the human superior parietal cortex (SPC) is subdivided into 4 parts (Fig. 1): 1) the superior parietal lobule (SPL) is framed anteriorly by the postcentral sulcus (PoCS), posteriorly by the lateral extension of the parieto-occipital sulcus (POS), and laterally by the intraparietal sulcus (IPS); 2) the medial wall of the IPS; 3) the posterior part of the paracentral lobule (PCL) is located medially, posterior to the medial extension of the central sulcus (CS), and dorsal and anterior to the posterior cingulate sulcus (CiS); and 4) the precuneus (PrC) is also located medially, but caudal of the CiS, which separates it from the PCL. Its posterior border is the POS, and its ventral border the subparietal sulcus (SuPS).

The human SPC and IPS play a key role in cognitive processes, in particular somatosensory and visuomotor integration as well as visuospatial attention and memory (for review, see Culham et al. 2006; Iacoboni 2006). These functions implicate, however, distinct subregions with differential preference (Lim et al. 1994; Allison et al. 1996; Sakakibara et al. 1999; Raichle et al. 2001; Grefkes et al. 2004; Simon et al. 2004; Stoeckel et al. 2004; Grefkes and Fink 2005; Cavanna and Trimble 2006; Culham et al. 2006; Iacoboni 2006; Northoff et al. 2006; Orban et al. 2006; Sereno and Huang 2006; Wenderoth et al. 2006; Fiehler et al. 2007; Hagler et al. 2007; Molenberghs et al. 2007). It is likely that a complex mosaic of structurally distinct microanatomical areas in the human SPC and IPS underlies this functional heterogeneity. In addition to specializations within the SPC and IPS, structural and functional differences between hemispheres and genders have been reported which are, however, still under debate (Kennedy et al. 1998; Grön et al. 2000; Gur et al. 2000; Unterrainer et al. 2000, 2005; Dietrich et al. 2001; Good et al. 2001b; Watkins et al. 2001; Allen et al. 2002, 2003; Jordan et al. 2002; Weiss et al. 2003; Boghi et al. 2006; Cavanna and Trimble 2006; Culham et al. 2006; Halari et al. 2006; Luders et al. 2006; Ohnishi et al. 2006; Barrick et al. 2007; Gorbet and Sergio 2007).

In his widely used cytoarchitectonic map (Fig. 2), Brodmann (1909) parcellated the SPC into area 5 anteriorly, located on the posterior PCL and anterior SPL, and area 7 more posteriorly on the SPL and the PrC (later he subdivided area 7 into anterior area 7a and posterior area 7b; Fig. 2; Brodmann 1914). In other less frequently used maps, however, parcellations were suggested that were considerably different with respect to the number and location of areas (Vogt 1911; von Economo and Koskinas 1925; Gerhardt 1940; Sarkisov et al. 1955; Batsch 1956). Reasons for these discrepancies include different histological staining techniques, different subjective criteria for the delineation of microanatomical areas, and sample sizes that were too small to account for the considerable interindividual anatomical variability of the human brain (Zilles et al. 2002, 2003; Uylings et al. 2005).

Oriented on macroanatomical landmarks, Talairach and Tournoux (1988) transferred Brodmann's 2D schematic drawings to their 3D stereotaxic atlas, which is frequently used as anatomical reference in functional imaging experiments. However, this atlas cannot be used to reliably assign functional activations to cytoarchitectonic areas because the precision of the transformation from Brodmann's drawings to the stereotaxic atlas is unknown. Furthermore, this atlas does not account for the considerable interindividual anatomical variability of the human brain. This variability makes it impossible to estimate the precise location of cytoarchitectonic areas and their borders from macroanatomical structures like gyri or sulci (Geyer et al. 1996, 1999; Amunts et al. 1999; Grefkes et al. 2001; Morosan et al. 2001; Zilles et al. 2002; Uylings et al. 2005; Caspers et al. 2006; Choi et al. 2006; Eickhoff, Amunts, et al. 2006a; Eickhoff, Schleicher, et al. 2006c; Malikovic et al. 2007; Rottschy et al. 2007; Scheperjans et al. 2007). Another drawback is that the abovementioned detailed functional pattern of areas in the SPC and IPS is not reflected in sufficient

detail by Brodmann's (1909, 1914) cytoarchitectonic bipartition (Fig. 2) and hence also not in the atlas of Talairach and Tournoux (1988).

Recently, based on multimodal analysis of cyto- and receptorarchitecture in postmortem brains, a new parcellation of the human SPC was suggested, comprising 8 distinct microanatomical areas (Scheperjans, Grefkes, et al., 2005; Scheperjans, Palomero-Gallagher, et al. 2005, Scheperjans et al. 2007). Three of these areas were delineated in the region of Brodmann's area (BA) 5 (5Ci, 5M, 5L), 4 were found in the region of BA 7 (7PC, 7A, 7P, 7M), whereas area hIP3 was described in the anterior part of the medial wall of the IPS (amIPS). Consequently, the new parcellation (Scheperjans, Grefkes, et al., 2005; Scheperjans, Palomero-Gallagher, et al. 2005, Scheperjans et al. 2007) considerably extends and modifies that of Brodmann (1909, 1914; Fig. 2) by introducing further subdivisions of BAs 5 and 7 and by defining a new cytoarchitectonic area (hIP3) in the amIPS. Additionally, our recent cytoarchitectonic study (Scheperjans et al. 2007) has important methodological advantages compared with previous anatomical investigations (Brodmann 1909, 1914; Vogt 1911; von Economo and Koskinas 1925; Gerhardt 1940; Sarkisov et al. 1955; Batsch 1956). An observer-independent approach was used for the detection of cytoarchitectonic borders, and each area was mapped in 10 postmortem brains to account for interindividual anatomical variability (Schleicher et al. 1999, 2000, 2005; Amunts and Zilles 2001; Zilles et al. 2002).

In the present study, we used this cytoarchitectonic parcellation of the human SPC (Scheperjans et al. 2007) together with established techniques for spatial normalization and image processing (Henn et al. 1997; Hömke 2006) to calculate 3D probabilistic maps and a maximum probability map (MPM) of this region in the stereotaxic reference space of the Montreal Neurological Institute (MNI; Evans et al. 1992; Amunts and Zilles 2001; Mazziotta et al. 2001; van Essen 2004; Eickhoff et al. 2005). Furthermore, we looked for anatomical correlates of observed functional/behavioral differences. The topographical relations between the areas were investigated based on the probability of mutual borders and on the comparison of their stereotaxic centers of gravity and volumes (Amunts et al. 2007). The data were further analyzed with respect to systematic differences between hemispheres or genders and with respect to the intersubject anatomical variability.

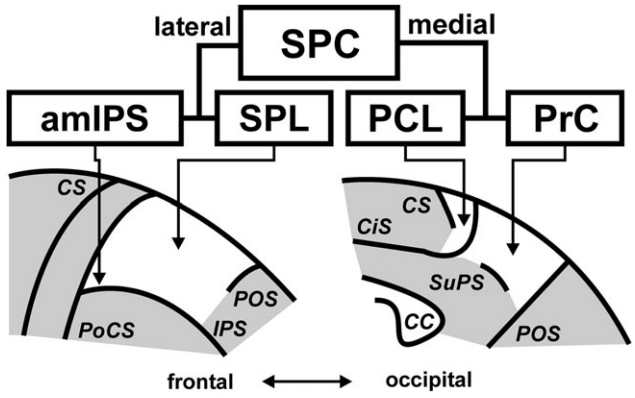

Figure 1. Schematic drawing of the lateral and medial aspects of a human hemisphere focused on the parietal region. The topography of the 4 different examined macroanatomical parts of the SPC (white area) is demonstrated: SPL, anterior part of the medial wall of the IPS (amIPS), posterior PCL, and PrC. CC, corpus callosum.

Materials and Methods

Cytoarchitectonic Mapping and 3D Reconstruction

Twelve human postmortem brains (6 male, 6 female, age range 37–86 years) were histologically processed (Table 1), and 8 areas were delineated in the SPC using an observer-independent algorithm for the detection of cytoarchitectonic borders (for details, see Schleicher et al. 1999; Scheperjans et al. 2007). Due to artifacts in the histological sections of some brains, the samples analyzed for area 7M differed from those of the other areas. Eight brains were analyzed with respect to all areas, 2 were analyzed for area 7M only, and 2 were analyzed for all areas except area 7M. Thus, each area was mapped in 10 brains.

The locations of each area, including layers I–VI, were interactively labelled in high-resolution scans (1200 dpi; ~20 μm/pixel; 8 bit gray value resolution) of the respective equidistant histological sections (Fig. 3; section thickness = 20 μm; section spacing 0.9–1.2 mm). The brains and representations of the areas were 3D reconstructed (Fig. 4) using 1) the high-resolution scans of the histological sections providing detailed anatomical information, but with strong deformation and no spatial reference, and 2) a structural magnetic resonance imaging 3D volume data set (3D FLASH sequence, flip angle = 40°, repetition time TR = 40 ms, echo time TE = 5 ms, 128 sagittal sections, spatial resolution 1 × 1 × 1.17 mm, 8 bit gray value resolution) obtained between fixation and embedding of the respective brain with only minor deformations but lower spatial resolution (Hömke 2006).

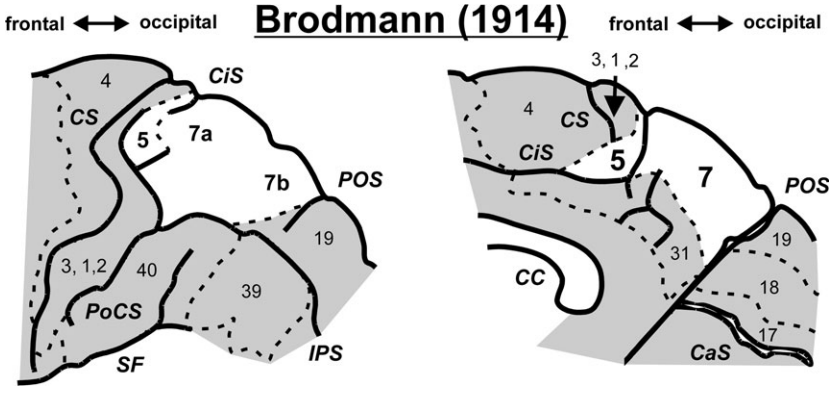

Figure 2. Modified schematic drawings of the lateral (left) and medial (right) aspects of the map of Brodmann (1914) with emphasis on his parcellation of the SPC (white area). Dashed lines indicate the borders of the cortical areas. CaS, calcarine sulcus; CC, corpus callosum; SF, sylvian fissure.

Table 1
Brains used for analysis of the SPC

Brain no.	Sex	Age (years)	Fresh volume (cm^3)
146/86	Male	37	1392
16/96[a]	Male	54	1703
189/92[b]	Male	56	1231
2/95	Female	85	1014
207/84	Male	75	1307
2431	Male	39	1196
281/93	Male	69	1318
340/83[b]	Female	79	1352
544/91[a]	Female	79	1308
56/94	Female	72	1178
68/95	Female	79	1076
71/86	Female	86	1078

[a]Analyzed for area 7M only.
[b]Not analyzed for area 7M.

Spatial Normalization and Probabilistic Maps

The reconstructed postmortem brains were subsequently spatially normalized to the T1-weighted single-subject template of the MNI (Evans et al. 1992) using a nonlinear elastic registration algorithm (Henn et al. 1997; Hömke 2006). Because the origin of the MNI reference space is located 4 mm more caudally (*y*-axis) and 5 mm more dorsally (*z*-axis) than the anterior commissure of this specific template brain, the data were shifted by this offset to "anatomical MNI space" (Amunts et al. 2005). Hereby, the anterior commissure was maintained as the anatomical reference of the coordinate system.

The representations of each delineated cytoarchitectonic area from the individual brains were then superimposed in this common reference space. Thereafter, probabilistic maps were calculated for each area by assigning frequency values (0/10–10/10) to each voxel of the reference brain quantifying the local degree of overlap (i.e., probability) across the 10 postmortem brains. For visualization of these maps, 1st the border between gray and white matter was determined from the volume data set of the MNI single-subject template and the triangulated white matter surface was calculated (Fig. 5: RAW; ~10^5 vertices per hemisphere; average distance between neighbouring vertices = 1.05 ± 0.2 mm; BrainVISA; Mangin et al. 2004). Secondly, the white matter surface and the Gaussian filtered (standard deviation [SD] = 2 mm) volume data set of each probabilistic map were superimposed. The overlap of the nearest voxel of the map was assigned to each vertex of the surface, and this overlay was subsequently median filtered. To reveal the topography of the map within the sulci, the surface was inflated up to a point where most sulci were flattened and where only major anatomical structures were still visible (Fig. 5: INFLATED; BrainVISA; Mangin et al. 2004). Vertex points with overlaps between 3/10 and 10/10 were color coded (Fig. 5).

Maximum Probability Map

To generate a contiguous, nonoverlapping parcellation of the SPC, an MPM (Eickhoff et al. 2005; Eickhoff, Heim, et al. 2006) was calculated from the probabilistic maps of the 8 areas as well as previously mapped areas of the surrounding precentral (BA 4), postcentral (areas 3a and 3b, BAs 1 and 2), and intraparietal (hIP1 and hIP2) cortex (Geyer et al. 1996, 1999; Grefkes et al. 2001; Choi et al. 2006). This map was computed by comparing the probabilities for each area (i.e., the counts of overlapping representations) in each voxel and assigning that voxel to the cytoarchitectonic area with the highest probability (Eickhoff et al. 2005). If areas showed equal probabilities, the respective voxel was assigned to the area with the higher average probability in the 26 directly adjacent voxels. In regions with no overlap of at least 2 probabilistic maps (e.g., at borders to yet unmapped regions), only voxels with a frequency value of at least 4/10 were included in the MPM (Eickhoff et al. 2005). It is important to note that the MPM does not show the parcellation or cytoarchitectonic borders of an exemplary or typical hemisphere as do classical architectonic brain maps (e.g., Brodmann 1909) but reflects in each voxel of the reference brain the most likely area from a sample of 10 postmortem brains. Furthermore, it provides a better representation of the true volumes of the included areas than a combination of thresholded probabilistic maps (Eickhoff et al. 2005; Eickhoff, Heim, et al. 2006). The surfaces of the MPM and of the white matter of the template brain were reconstructed, superimposed, and visualized (Figs. 6–9) using Amira 4.1.0 (Mercury Computer Systems, Inc, Chelmsford, MA).

Analysis of Cytoarchitectonic Borders

We investigated the topographical relations of the cytoarchitectonic areas and their variability by analyzing the probability of mutual borders (Table 2). This analysis supplements previously published data concerning the precise location of these borders with respect to anatomical landmarks (Scheperjans et al. 2007). The patterns of areas of the individual brains were visualized using Amira 4.1.0 (Mercury Computer Systems, Inc) and used together with the scanned histological sections for evaluation of the hemispheres (Table 2 and Figs. 3 and 4). Topographical relations between area 7M and the remaining areas of the SPC were examined in the subsample in which all 8 areas had been delineated (16 hemispheres). Topographical relations between the areas of the SPC and the surrounding cortex were examined in the subsample (14 hemispheres) that had previously been used for the delineation of adjacent areas as well (4, 3a, 3b, 1, 2, hIP1, and hIP2; Geyer et al. 1996, 1999; Grefkes et al. 2001; Choi et al. 2006). To look for interhemispheric differences in the pattern of mutual borders, we tested for each border that was present in some, but not all, hemispheres for the independence between the hemisphere and the probability with which the border was present. Therefore, we used 2-by-2 contingency tables and Fisher's exact test (2 tailed; significance level $P < 0.05$).

Analysis of Stereotaxic Centers of Gravity

Furthermore, the topographical relations were analyzed based on stereotaxic centers of gravity that were calculated for each area and hemisphere after spatial normalization (Table 3). Differences of the absolute values of the coordinates (means across right and left hemispheres) between areas (Fig. 10) were tested for significance separately for each axis using pairwise permutation tests. For each of these tests, the 20 values were 1st grouped according to their true label (10 for area x and area y, respectively) and a contrast estimate was calculated between the means of these groups. The null distribution was estimated by Monte-Carlo simulation. The 20 values were randomly redistributed into 2 groups, the same contrast was calculated, and this procedure was repeated for 100 000 iterations. The difference between the 2 areas was considered significant if the contrast estimate of the true comparison was larger than 95% of the values under random (i.e., null) distribution ($P < 0.05$; Eickhoff et al. 2007). The calculated centers of gravity were subsequently also compared with those of the MPM (Table 3).

The calculation of the probabilistic maps and of the stereotaxic centers of gravity used for the pairwise comparisons between areas (Table 3 and Fig. 10) was based on the nonlinear elastic registration of the individual postmortem brains to the reference brain (see above). This algorithm largely reduces intersubject differences of brain shape and size and removes nonlinear distortion caused by histological processing. However, it can influence interhemispheric differences of the individual postmortem brains, by introducing shape asymmetries that are determined by the asymmetry of the target brain, that is, the reference brain (Amunts et al. 2000). For this reason, we used the data sets from the individual postmortem brains after a linear affine registration to the reference brain for the analysis of interhemispheric and gender-specific influences on the stereotaxic centers of gravity. This registration reduced intersubject variability in brain size and position but did not affect interhemispheric asymmetries (Amunts et al. 2000). For each area and axis, differences of the absolute coordinates were tested for significant effects of hemisphere and gender, as well as of the interaction of these factors using the permutation test.

Topographical variation in stereotaxic location was quantified for each area, hemisphere, and axis by the SD of the coordinates of the

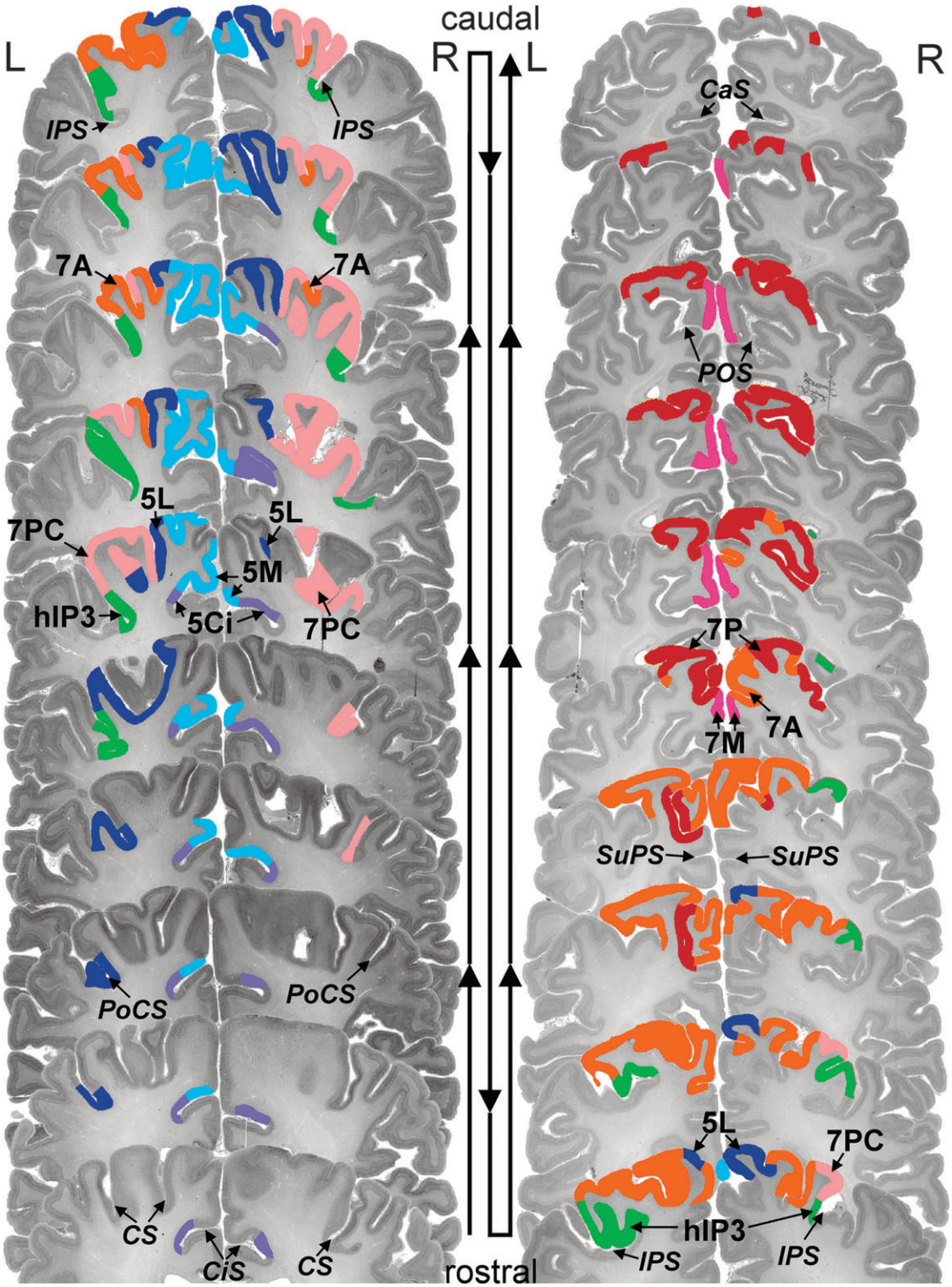

Figure 3. Scanned silver-stained histological coronal sections (thickness = 20 μm; each 120th section; section spacing = 2.4 mm) from a postmortem brain with superimposed colored representations of the delineated cytoarchitectonic areas of the SPC. The sections are aligned in 2 columns from the most rostral section in the bottom left corner to the most caudal section in the top right corner. CaS, calcarine sulcus.

centers of gravity (Table 3 and Figs. 10 and 11). Differences in the stereotaxic variance between areas (derived from mean absolute coordinates across hemispheres after nonlinear registration) were tested for each axis across both hemispheres, using pairwise permutation tests as described above. The permutation test was likewise applied to test differences in variance for significant effects of hemisphere and gender, as well as of the interaction of these factors (after linear registration).

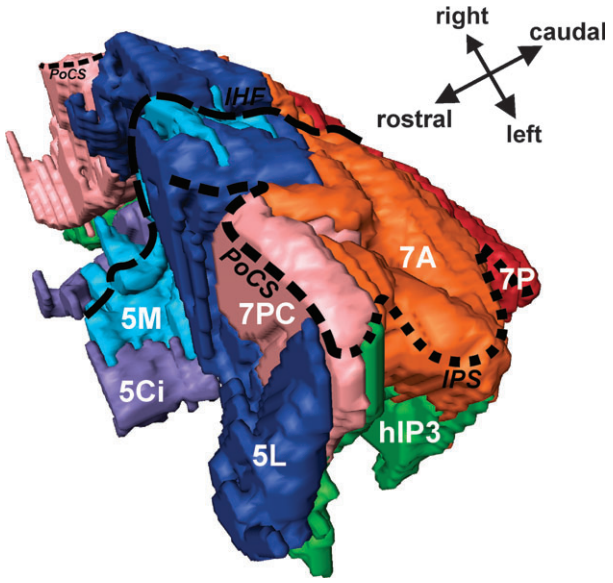

Figure 4. 3D reconstruction of the cytoarchitectonic areas of the SPC of the same brain based on the representations from Figure 3. Smoothing was largely reduced to give an impression of the arrangement of the individual histological sections. The point of view is left-anterior and focused on the junction between the left PoCS and IPS. Dashed lines demarcate the interhemispheric fissure (IHF) and the rims of the sulci. Note the complex shape of the areas, particularly in the walls of the sulci, and the lateral extension of left area 5L reaching up to area hIP3 at the junction of the PoCS and IPS.

Volumetry

The fresh total volume of each brain was estimated from its fresh weight and a mean density of 1033 kg/m^3 (Table 1; Kretschmann and Wingert 1971). The volume after histological processing (histological volume) was calculated based on area measurements of the brain tissue in the digitized histological sections (Amunts et al. 2005). To compensate for shrinkage due to histological processing, an individual correction factor was defined for each postmortem brain as the ratio between its fresh volume and its histological volume (mean: 2.01; range: 1.47–2.45). The fresh volume (Fig. 12) of each cytoarchitectonic area was stereologically estimated in each hemisphere using the delineations in the digitized histological sections (Fig. 3), Cavalieri's principle, and the correction factor (Uylings et al. 1986; Amunts et al. 1999, 2005, 2007). Because male brains (1357 ± 183 cm^3) were on average 16% larger than female brains (1168 ± 137 cm^3), the volume of each area in each brain was expressed as a fraction of total brain volume to avoid a confounding influence of total volume (Table 1). Pairwise permutation tests were used to test differences of the volume fraction between areas (means of right and left hemispheres). For each area, differences of the volume fraction were tested for significant effects of hemisphere and gender, as well as of the interaction of these factors using the permutation test.

For each area, interindividual variability of its volume fraction was quantified by the coefficient of variation (CV = SD/mean) separately for hemispheres and genders (Fig. 12). Pairwise permutation tests were used to test CV differences between areas (derived from mean volume fractions across hemispheres) for significance. Likewise, permutation tests were used for each area to test differences in the CV for significant effects of hemisphere and gender and of the interaction of these factors.

For the present study, very high standards were installed concerning the quality of the tissue and the medical history of the donors (e.g., short postmortem delay, no neurological or psychiatric diseases, and high quality of histological preparations). The application of these strict criteria, which are an important prerequisite for the precise analysis of cortical architecture, limits the availability of suitable brains, and it was therefore not possible to use age-matched samples for both genders. Thus the question arises, whether our analysis of gender differences is confounded by age. Several studies have shown that age effects on cortical anatomy in the SPC are much weaker than for example in the frontal lobe (Raz et al. 1997; Moore et al. 2005). Furthermore, the age-related decrease of cortical volume in the SPC is mainly related to the decrease of total brain volume (Good et al. 2001a). In particular, the latter observation is critical for the evaluation of our data, as in the present study all volumetric data were normalized to total brain volume before analysis.

To test whether in the present analysis age differences had a confounding effect on our analysis of gender differences, we tested for a correlation between the volume fraction and age. For none of the cytoarchitectonic areas, a significant correlation was observed. The mean Fisher's z from both hemispheres was $\bar{z} = 0.30 \pm 0.19$ corresponding to a mean Pearson's correlation coefficient of $\bar{r} = 0.29$. Also in our preceding study (Scheperjans et al. 2007), which was performed on the same sample of brains, none of the investigated histological parameters showed a significant correlation with age. Hence, although we cannot completely exclude a confounding effect of age on our analysis of gender differences, it can be estimated that this effect is very small.

Results

Probabilistic Maps and MPM

Figure 5 shows the color-coded probabilistic maps for each area overlayed onto the inflated white matter surface of the MNI single-subject template brain. Due to the high interindividual anatomical variability, voxels/vertices in the periphery of the maps with low overlap (i.e., probabilities; blue) were more frequent than central voxels/vertices with high overlap (red). Therefore, the maps of different areas overlapped considerably at lower frequencies.

A nonoverlapping parcellation of the SPC was obtained by combining the individual probabilistic maps and creating an MPM that showed a pattern of areas similar to those of the individual brains (Figs. 4 and 6–9; see below). On the lateral surface, the most anterior areas were 5L and 7PC occupying large parts of the posterior wall of the PoCS (Figs. 6–8). Area 5L extended to the postcentral gyrus and also medially to the posterior PCL and CiS (Figs. 6–8). Area 7PC reached to the superficial part of the amIPS in both hemispheres (Figs. 6–8). On the medial surface, area 5M was located ventral to area 5L on the posterior PCL and in the CiS (Figs. 6 and 9). Area 5Ci was located deeper inside the CiS than area 5M and extending more anteriorly (Figs. 6 and 9) having borders with the cingulate cortex. On the lateral surface, area 7A was abutting areas 5L and 7PC posteriorly, reaching to the posterior wall of the PoCS on the left. Bilaterally, it extended to superficial parts of the medial wall of the IPS and to the PrC with borders to areas hIP3 and 7M and the posterior cingulate cortex, respectively (Figs. 6–8). Its posterior border was to area 7P that also extended to the medial wall of the IPS and to the PrC, bordering area 7M bilaterally and the posterior cingulate cortex on the left (Figs. 6–8). Area 7M occupied the posterior ventral PrC and did not reach to the lateral surface (Fig. 6). Medial parts of BA 7 were represented dorsal and ventral to the SuPS (Fig. 6). Posteriorly, areas 7P and 7M extended to superficial parts of the anterior wall of the POS (Figs. 6–8). In the amIPS, area hIP3 was located near the junction with the PoCS and had medial borders to areas 7PC and 7A (Figs. 6 and 8).

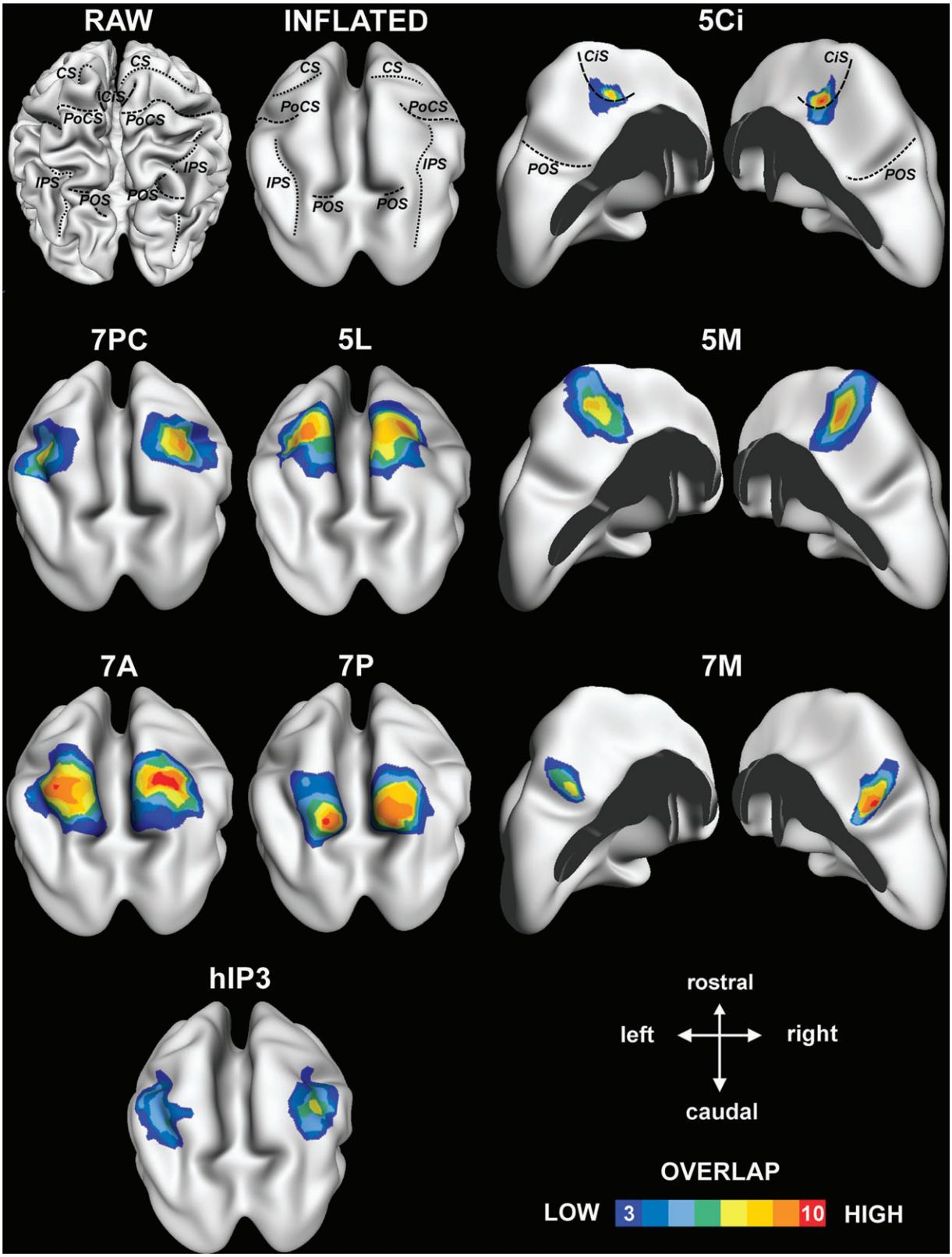

Figure 5. Probabilistic maps of the delineated areas visualized as overlays on the white matter surface of the template brain (RAW) that was subsequently inflated (INFLATED). Except for areas 5Ci, 5M, and 7M, the point of view is posterior with an elevation of 45° from the horizontal plane. For areas 5Ci, 5M, and 7M, the point of view is less elevated and the left and right hemispheres were separated so that the medial brain surface is shown. The degrees of overlap across the 10 postmortem brains (3/10–10/10) are color coded showing vertices with low overlap in blue and those with high overlap in red. The major sulci are marked by dashed lines in the top row.

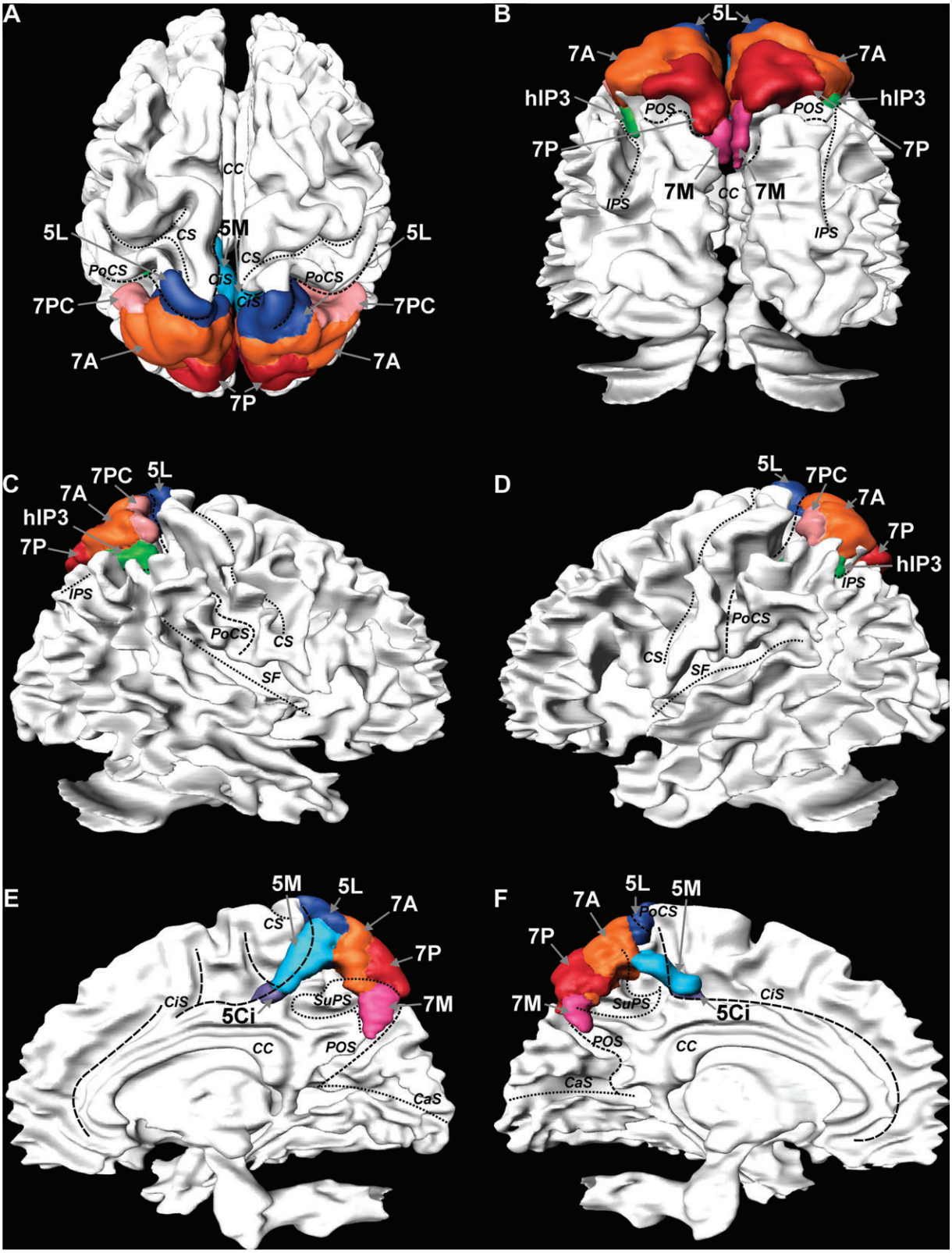

Figure 6. Surface reconstruction of the white matter of the template brain with the superimposed MPM of the SPC. The major sulci are marked by dashed lines. (*A*) Dorsal view with the frontal poles on the top and the occipital poles on the bottom. (*B*) Posterior view. (*C*, *D*) Lateral views of the right (*C*) and left (*D*) hemisphere. (*E*, *F*) Medial views of the separated right (*E*) and left (*F*) hemisphere. CaS, calcarine sulcus; CC, corpus callosum; SF, sylvian fissure.

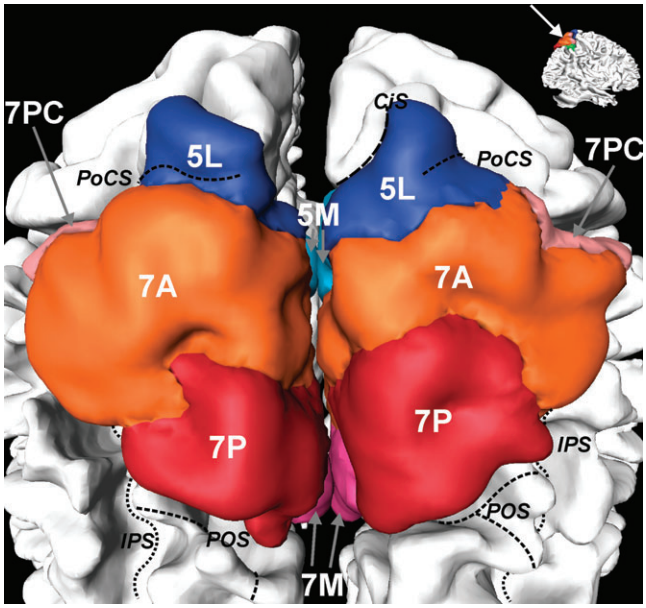

Figure 7. Surface reconstruction of the white matter of the template brain with the superimposed MPM of the SPC. The point of view is posterior with an elevation of 45° from the horizontal plane as shown by the arrow in the inset in the right upper corner. The major sulci are marked by dashed lines.

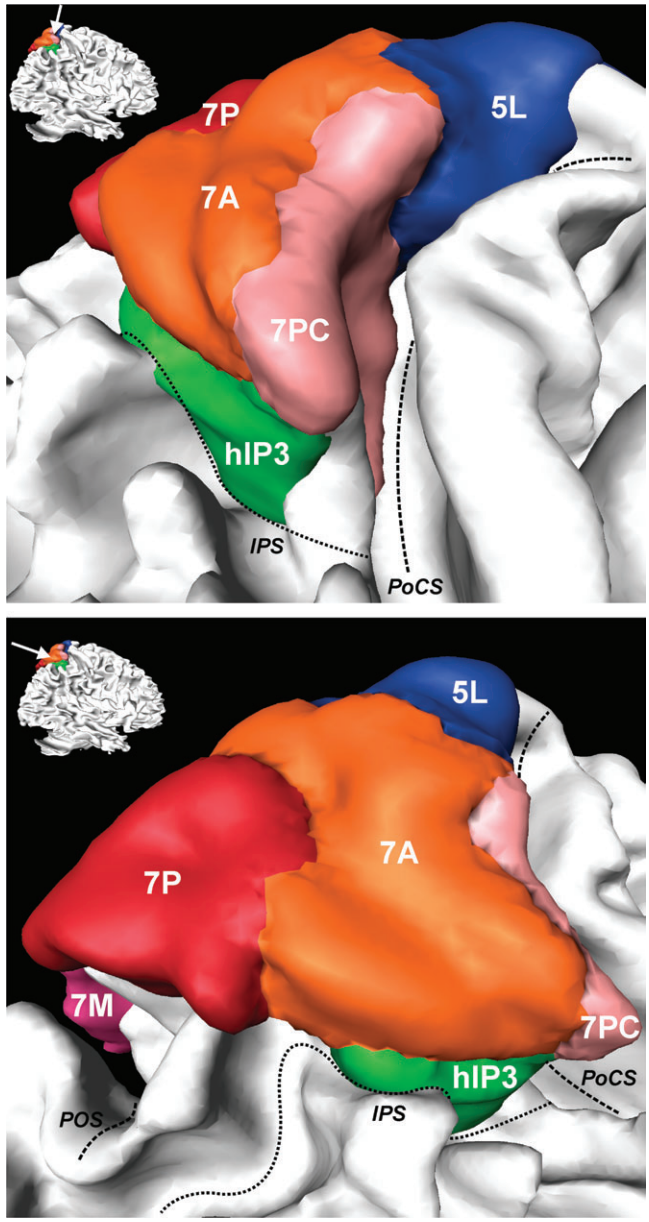

Figure 8. Surface reconstruction of the white matter of the right hemisphere of the template brain with the superimposed MPM of the SPC. The focus is on the IPS. The major sulci are marked by dashed lines. The point of view of the upper image is anterior lateral, as shown by the arrow in the inset in the upper left corner, so that the junction between the PoCS and the anterior part of the IPS is shown. The point of view of the lower image is posterior lateral, as shown by the arrow in the inset in the upper left corner, so that the posterior part of the IPS and the lateral branch of the POS are shown.

Analysis of Intersubject Variability and Interhemispheric Asymmetry of Cytoarchitectonic Borders

Several borders were present in all hemispheres (5Ci/5M, 5M/5L, 5L/7PC, 7PC/7A, 7A/7P; Table 2 and Figs. 3 and 4) and also represented in the MPM (see above; Figs. 6–9). Area 5L also frequently had a border to area 7A (85%; Table 2). Area 7P bordered area 7M in all but 1 hemisphere (94%; Table 2), when a posterior extension of area 7A separated these 2 areas. Area hIP3 very frequently had a border to areas 7PC and 7A (95% and 90%, respectively; Table 2) but rarely to area 7P (10%; Table 2). However, considerable variations were observed between subjects and hemispheres as, for example, the border between areas 5M and 5L could be located on the medial or lateral surface of the hemisphere (Figs. 3, 4, and 6; cf. Scheperjans et al. 2007). Between individual hemispheres, such differences of the location of areas led to differences in the pattern of interareal borders. For this reason, several borders were found with lower probabilities in the sample, for example, in only 25% of the hemispheres area 5L extended laterally up to the junction of the PoCS and IPS and had a border with area hIP3 (Table 2 and Figs. 3 and 4).

Considerable intersubject variability was also present with respect to the topographical relations between the areas of the SPC and the surrounding cortex (Table 2). Only the anterior border of area 5M to the motor cortex (BA 4), the posterior borders of areas 7P (laterally) and 7M (medially) to the parieto-occipital cortex, and the medial ventral borders of areas 5Ci (anterior) and 7M (posterior) to the cingulate cortex (aCi: ventral to the PCL; pCi: ventral to the PrC) were present in all hemispheres (Table 2). Frequent borders to the somatosensory cortex (Table 2) were found between areas 5M and 3a/3b (86%/79%) and between areas 5L and 2 (86%). In the IPS, area hIP3 had almost always a border with area hIP2 (93%) but only in half of the hemispheres with area hIP1 (Table 2). Medial ventral borders to the posterior cingulate cortex were frequently found (Table 2) for areas 7A (95%) and 7P (80%).

No significant effect of hemisphere on the probability of any border was found ($P > 0.05$; 2-tailed Fisher's exact test).

Analysis of Stereotaxic Centers of Gravity

The mean stereotaxic coordinates of the centers of gravity of the areas across the individual brains are shown in Figure 10 (means of right and left coordinates) and Table 3. Despite considerable interindividual variations, the relative positions of the delineated areas in the SPC were similar across subjects;

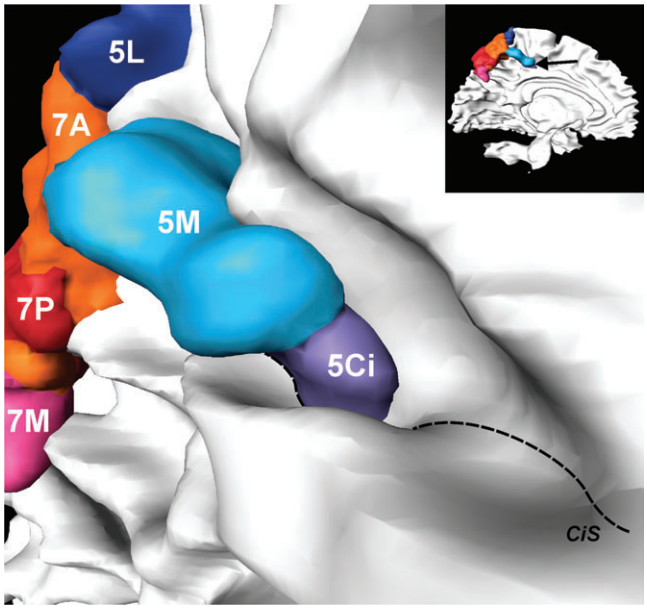

Figure 9. Surface reconstruction of the white matter of the left hemisphere of the template brain with the superimposed MPM of the SPC. The focus is on areas 5M and 5Ci in the CiS. The fundus of the CiS is marked by a dashed line. The point of view is on the medial surface of the frontal lobe slightly dorsal to the CiS, as shown by the arrow in the inset in the upper right corner. Note that area 5Ci lies deeper in the dorsal wall and fundus of the CiS and extends more anterior than area 5M.

Table 2

Probabilities of cytoarchitectonic borders as a fraction of the total number of hemispheres examined for that border ($14 \leq n \leq 20$; see text)

	5Ci	5M	5L	7PC	7A	7P	7M	HIP3
5M	100%							
5L	20%	100%						
7PC	0%	30%	100%					
7A	10%	10%	85%	100%				
7P	0%	0%	0%	0%	100%			
7M	0%	0%	0%	0%	25%	94%		
hIP3	0%	0%	25%	90%	85%	10%	0%	
BA 4	36%	100%	14%	0%	0%	0%	0%	0%
Area 3a	0%	86%	21%	0%	0%	0%	0%	0%
Area 3b	0%	79%	57%	0%	0%	0%	0%	0%
BA 1	0%	29%	50%	14%	0%	0%	0%	0%
BA 2	0%	36%	86%	57%	0%	0%	0%	36%
hIP1	0%	0%	14%	14%	0%	0%	0%	50%
hIP2	0%	0%	21%	21%	0%	0%	0%	93%
POC	0%	0%	0%	0%	5%	100%	100%	0%
aCi	100%	75%	30%	0%	0%	0%	0%	0%
pCi	5%	35%	60%	15%	95%	80%	100%	0%

for example, area 5M was always located medial to area 5L (Figs. 4 and 7), and the centers of gravity of all areas differed significantly from each other in at least 2 dimensions. Focusing on the areas that very frequently had borders to each other (see above; Table 2), the following spatial relations were confirmed by significantly different coordinates (Table 3 and Fig. 10): area 5Ci was lateral, anterior, and ventral to area 5M (i.e., area 5Ci was located deeper in the CiS); area 5M was medial, anterior, and ventral to area 5L; area 5L was medial and dorsal to area 7PC; area 7A was lateral, posterior, and ventral to area 5L and medial and posterior to area 7PC; area 7P was medial, posterior, and ventral to area 7A; area 7M was medial and ventral to area 7P; and area hIP3 was lateral and ventral to areas 7PC and 7A (i.e., area hIP3 was located deeper in the amIPS), posterior to area 7PC, and anterior to area 7A. These spatial relations can

Table 3

Coordinates (mm) of the stereotaxic centers of gravity in anatomical MNI space from the individual postmortem brains after nonlinear elastic registration to the reference brain (INDIV) and from the MPM

		Left						Right					
		X	SD	Y	SD	Z	SD	X	SD	Y	SD	Z	SD
5Ci	INDIV	−13	2	−40	5	51	4	10	3	−40	4	53	4
	MPM	−15		−39		49		12		−38		50	
5M	INDIV	−9	2	−45	5	63	6	6	3	−46	3	64	6
	MPM	−8		−46		59		6		−49		63	
5L	INDIV	−19	6	−51	7	68	5	15	3	−53	4	72	5
	MPM	−16		−51		73		13		−55		73	
7PC	INDIV	−31	5	−51	5	64	4	28	5	−52	5	64	5
	MPM	−34		−53		61		30		−52		61	
7A	INDIV	−21	3	−64	5	64	5	20	4	−64	3	66	4
	MPM	−19		−65		64		20		−65		64	
7P	INDIV	−11	3	−76	6	55	6	14	3	−75	2	59	3
	MPM	−9		−79		54		15		−77		59	
7M	INDIV	−3	1	−77	5	42	6	4	1	−74	3	42	5
	MPM	−1		−76		41		5		−75		42	
hIP3	INDIV	−34	6	−54	7	53	5	32	4	−56	7	56	6
	MPM	−32		−55		49		34		−56		51	

thus be regarded as a constant basic topographical pattern of areas in the SPC (Figs. 6–10). With the exception of the left X-coordinate of area 7M, all centers of gravity of the respective areas in the MPM were located within 1 SD of the mean coordinates across the individual centers of gravity (Table 3).

The permutation test revealed that the centers of gravity for areas 7P and 7M were located significantly more lateral in the right than in the left hemisphere. No significant effect of gender and no significant interaction were observed.

The analysis of the variance of the centers of gravity (Fig. 10) revealed no significant differences in the stereotaxic variation between the 8 areas in the pairwise comparisons. However, we observed significantly higher variation in the left hemisphere (y-axis: 7A and 7P) and in males (y-axis: 5M; z-axis: 5M, 7PC, 7A, 7P). A significant interaction of the factors hemisphere and gender was found for the variance of the X-coordinate of area 5Ci and of the Y-coordinate of area 5M (Fig. 11). For both areas, the variation was higher in the left hemisphere in males (Fig. 11). Particularly for area 5Ci, there was in addition higher righthemispheric variation in females (Fig. 11).

Volumetry

The average total volume fraction (% brain volume ± SD) of BAs 5 and 7 in those hemispheres that had been mapped with respect to all areas ($n = 16$) was 1.0055 ± 0.2614 (men: 1.0160 ± 0.3128; women: 0.9950 ± 0.2200; $P > 0.05$). Of the 8 delineated areas, the average volume fraction per hemisphere ($n = 20$) was largest for area 7A (0.3304 ± 0.2060) and smallest for areas 7M (0.0372 ± 0.0120) and 5Ci (0.0496 ± 0.0231). The remaining areas had intermediate volume fractions (5M: 0.1145 ± 0.0604; 5L: 0.1637 ± 0.0764; 7PC: 0.1270 ± 0.0843; 7P: 0.1522 ± 0.0665; hIP3: 0.1102 ± 0.0675). With respect to the mean volume fraction across hemispheres (Fig. 12: middle), area 7M was significantly smaller than area 5Ci and both were significantly smaller than all other investigated areas. Area 7A was significantly larger than all other areas. Furthermore, area 5L was significantly larger than areas 5M and hIP3. No significant differences of the volume fraction between hemispheres (Fig. 12: top) or genders (Fig. 12: middle) and no significant interaction were observed.

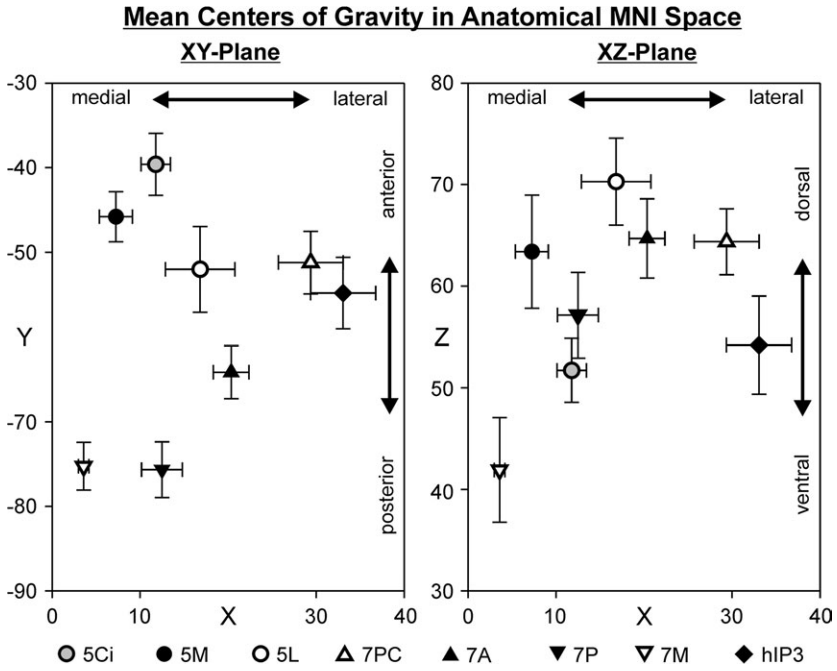

Figure 10. Scatter plots showing the mean coordinates (mm) and SDs of the centers of gravity in anatomical MNI space for the areas of the SPC calculated from the individual postmortem brains after nonlinear registration (means of left and right coordinates; absolute values for X-coordinates) in the horizontal (left) and coronal (right) planes ($n = 10$).

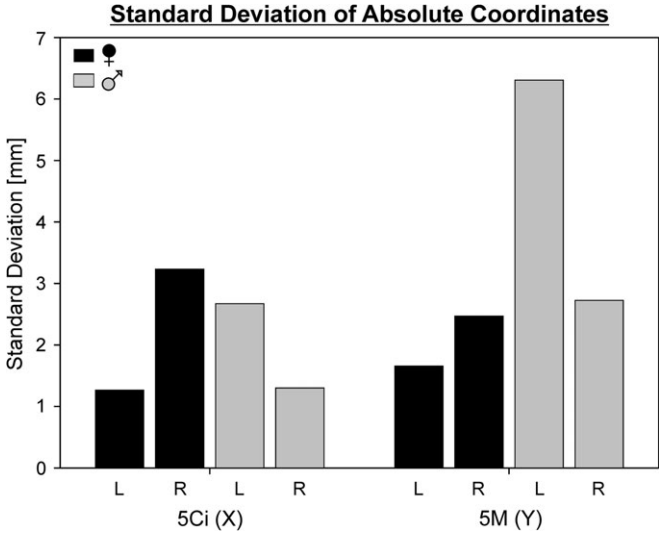

Figure 11. Bar diagram showing the SD of the absolute X-coordinate of area 5Ci and of the Y-coordinate of area 5M separately for men, women, and hemispheres. This measure of interindividual stereotaxic variation of the center of gravity was calculated from the individual brains after linear registration. The significant interaction of the factors hemisphere and gender (permutation test) was based on higher variation in the left hemisphere of males and in the right hemisphere of females ($n_f + n_m = 5 + 5$).

The volume fractions (% brain volume) of all areas showed strong variations between the 20 hemispheres, with the largest range (minimum-maximum; maximum/minimum) for area hIP3 (0.0129–0.2990; 23.14) and the smallest for area 7M (0.0198–0.0583; 2.94). Intersubject variations were quantified by the coefficients of variation (CV; Fig. 12: bottom). Based on the mean volume fractions across hemispheres, medial areas 5Ci and 7M showed relatively small variations compared with the remaining areas (Fig. 12: bottom). However, the differences between areas were not significant (Fig. 12: bottom). Neither a significant effect of hemisphere or gender nor an interaction was observed (Fig. 12: bottom). However, there was a trend toward higher variability in males for areas 5M, 5L, 7PC, 7A, and hIP3 (Fig. 12: bottom).

Discussion

In the present study, we analyzed topographical, stereotaxic, and volumetric data for 8 superior parietal cytoarchitectonic areas that were delineated by observer-independent techniques in a previous study (Scheperjans et al. 2007). We also provided probabilistic maps of these areas and an MPM of the SPC in standard MNI space.

Parcellation and Topographical Relations of Cytoarchitectonic Areas in Structure and Function

The SPC and IPS are involved in various cognitive processes, in particular somatosensory and visuomotor integration as well as visuospatial attention and memory (for review, see Culham et al. 2006; Iacoboni 2006). Reaching or pointing movements activate mainly anterior parts of the SPC when they are based predominantly on somatosensory information, whereas visual guidance implicates more posterior parts (Simon et al. 2004; Stoeckel et al. 2004; Wenderoth et al. 2006; Fiehler et al. 2007). A stronger representation of somatosensory information in the anterior areas of the SPL and of visual information in the posterior areas was also suggested by receptorarchitectonic findings (Scheperjans, Palomero-Gallagher, et al. 2005), showing that receptor distribution patterns in the anterior SPL are similar to those of the postcentral somatosensory cortex (BA 2), whereas patterns in posterior SPL resemble those of the extrastriate visual cortex (BA 19). Further supporting this segregation on the structural level is a study reporting that the

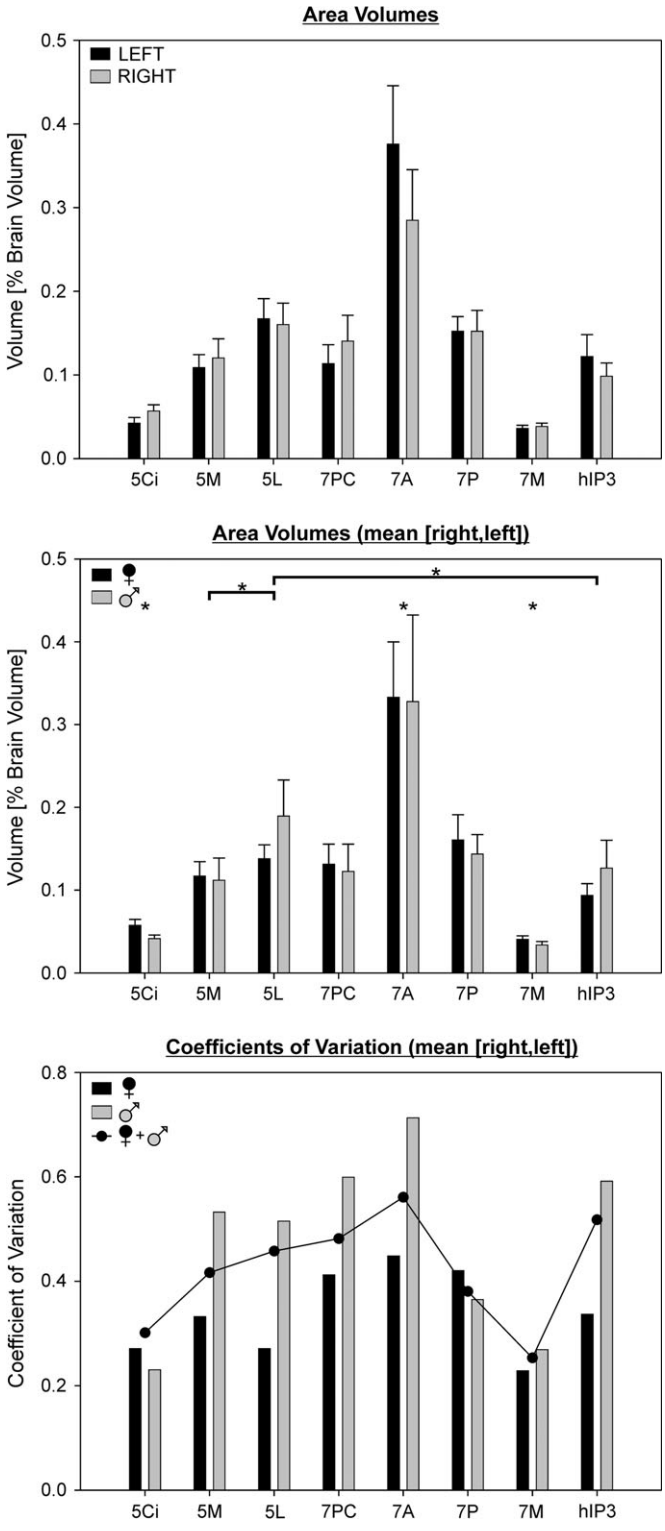

Figure 12. Results of the volumetric analyses. Top: Bar graph indicating the average volume of the individual areas relative to total brain volume separately for right ($n_r = 10$) and left hemispheres ($n_l = 10$). Error bars = standard error of the mean (SEM). Middle: Bar graph indicating the mean of right and left volumes of the individual areas relative to total brain volume separately for female ($n_f = 5$) and male ($n_m = 5$) subjects. Asterisks indicate the significantly different mean volume fractions (whole sample) of areas 5Ci, 7A, and 7M in comparison with all other areas and the significantly higher volume fraction of area 5L in comparison with areas 5M and hIP3. Error bars = SEM. Bottom: Bar graph indicating the CV of the mean of right and left volume fractions of the individual areas separately for male and female subjects ($n_f + n_m = 5 + 5$). The superimposed line plot indicates the CV across the whole sample ($n = 10$).

posterior SPL and medial wall of the IPS have a higher probability of fiber connections with the superior colliculus, a key structure for the control of eye movements, than the anterior SPL (Rushworth et al. 2006).

Anatomical and functional observations have suggested a similar rostrocaudal subdivision of the macaque SPC. The anterior SPC integrates mainly information from the somatosensory cortex (Pandya and Seltzer 1982) and provides the dorsal premotor cortex (PMd) with a spatial representation of the body parts (Mountcastle et al. 1975; Jones et al. 1978; Lacquaniti et al. 1995). The posterior SPC, in contrast, receives input from the visual cortex and is an important source of visual information for PMd in the context of visually guided reaching movements (Pandya and Seltzer 1982; Caminiti et al. 1996; Marconi et al. 2001; Battaglia-Mayer and Caminiti 2002). In both human and monkey SPC, however, visuospatial processing seems to be less regionally confined than somatosensory processing (Macaluso et al. 2003; Orban et al. 2006; Filimon et al. 2007; Hagler et al. 2007).

The abovementioned functional rostrocaudal bipartition in the human SPC supports Brodmann's (1909, 1914) parcellation into 2 main areas (Fig. 2), BA 5 (anterior) and BA 7 (posterior). While principally confirming this basic segregation, the present and the preceding studies (Scheperjans, Grefkes, et al. 2005; Scheperjans, Palomero-Gallagher, et al. 2005; Scheperjans et al. 2007) demonstrated a more complex pattern of 8 areas in the SPC (anterior: 5Ci, 5M, 5L, and 7PC; posterior: 7A, 7P, and 7M) and amIPS (hIP3). On the microstructural level, when both receptor- and cytoarchitectonic features are considered (Scheperjans, Grefkes, et al. 2005; Scheperjans, Palomero-Gallagher, et al. 2005; Scheperjans, et al. 2007), a gradual transition from anterior BA 5 to posterior area 7P, across areas 7PC and 7A, was observed. Although there was a strong anatomical variability in our sample (Figs. 5, 10, and 12), the stereotaxic centers of gravity of the delineated areas were well separated and several significant differences in the volume fraction were observed between areas (Table 3 and Figs. 10 and 12). In combination with the analysis of cytoarchitectonic borders (Table 2), which revealed that several borders were observed consistently across hemispheres and subjects, a constant basic topographical pattern of areas emerged, which was reflected in the MPM (Figs. 6–10).

The further subdivisions in the SPC described here thus extend the parcellation of this region beyond Brodmann's (1909) rostrocaudal bipartition into BAs 5 and 7. They correspond well to the more detailed pattern of functionally distinct areas recently demonstrated in humans and to structural and functional observations in macaque monkeys (Lewis and van Essen 2000; Simon et al. 2004; Grefkes and Fink 2005). Concerning the macaque SPC, recent studies have extended the initially proposed segregation between areas PE and PEc (Pandya and Seltzer 1982), arguing for an additional rostrocaudal gradient within area PEc (Marconi et al. 2001). These gradients might correspond to the structural transitions in the human SPC mentioned above. However, the areas of the human SPC are not simply arranged in a rostrocaudal sequence because area 7PC is located lateral to area 5L. In the macaque cortex, so far no area has been described that would topologically correspond to human area 7PC. However, by mapping topically organized sensory and visuomotor representations (Sereno and Huang 2006), a superior parietal area has been recently functionally identified in the human brain at

a location comparable to that of our area 7PC, which supports our parcellation.

Functional differences between areas of the SPL and IPS have been described, for example, for attentional processes. During the remapping of attentional priorities, a region in the anterior IPS is more implicated by endogenously guided attention shifts, as compared with exogenous shifts, than the SPL (Molenberghs et al. 2007), corroborating our definition of area hIP3 in the amIPS. Further supporting our structural parcellation in the medial wall of the IPS are reports about several functionally defined human intraparietal areas (e.g., DIPSM, DIPSA, hMIP, mIPS, IPS1–3; Grefkes et al. 2004; Grefkes and Fink 2005; Culham et al. 2006; Iacoboni 2006; Orban et al. 2006; Hagler et al. 2007) and about anatomically and functionally characterized areas PEip (anterior) and MIP (posterior) in the macaque brain (Matelli et al. 1998; Lewis and van Essen 2000; Grefkes and Fink 2005).

Functional dissociations between lateral (SPL) and medial (PCL, PrC) parts of the SPC have been reported as well. The anterior medial SPC, that is, the PCL, is the most important among parietal areas for micturition control (Sakakibara et al. 1999) and has sensorimotor functions (Lim et al. 1994; Allison et al. 1996), corroborating our cyto- and receptorarchitectonic findings of distinct areas (e.g., area 5M) in this region (Scheperjans, Grefkes, et al. 2005; Scheperjans et al. 2007). No mediolateral subdivisions have so far been described for area PE in the anterior macaque SPC that could be homologues of the here described areas 5L and 5M. However, the higher order sensorimotor area PEci in the macaque CiS might correspond to area 5Ci (Pandya and Seltzer 1982; Shima et al. 1991; Morecraft et al. 2004). In the more posterior SPC, there are functional differences between the SPL and PrC during visuospatial navigation (Grön et al. 2000; Ohnishi et al. 2006), and the PrC belongs to the so called cortical midline structures related to self-referential processing (Raichle et al. 2001; Cavanna and Trimble 2006; Northoff et al. 2006). This supports our observation of structural differences between the SPL and the PrC, namely the delineation of subarea 7M. Furthermore, this area lies at a location comparable to that of area PGm in the macaque brain (Pandya and Seltzer 1982).

Functional subdivisions within the PrC have been suggested with a focus on self-centered mental imagery and attentional processes in the anterior part and on episodic memory retrieval and saccade-related activity in the posterior part (Simon et al. 2004; Cavanna and Trimble 2006), which seems to be structurally reflected in our parcellation, namely anterior area 7A and more posterior areas 7P and 7M.

In line with the abovementioned structural and functional findings of multiple distinct areas, it has been shown that anatomical alterations and hypoactivations of circumscribed parts of the SPC and IPS are behaviorally relevant in certain disorders with central nervous system involvement (e.g., gray matter reduction in the posterior IPS and hypoactivation around the IPS and lateral SPL are related to visuospatial cognitive deficits in Williams syndrome; Meyer-Lindenberg et al. 2004; Eckert et al. 2005, 2006).

Although the here presented parcellation shows considerable similarities with current concepts of the macaque SPC, noteworthy differences were observed, for example, the mediolateral subdivisions in the anterior human SPC (subareas 5L, 5M, and 7PC). Future structural and/or functional studies may elucidate, whether homologues of these subareas can be identified also in nonhuman primates or whether they are human specific. It is likely that the cytoarchitectonic areas presented in this study are structural correlates of complex functional segregations in the human SPC and IPS (Figs. 6–9; Scheperjans, Grefkes, et al., 2005; Scheperjans, Palomero-Gallagher, et al. 2005; Scheperjans et al. 2007). The probabilistic maps of these areas in stereotaxic space constitute an objective anatomical reference and can now be integrated into functional imaging experiments to explore in detail the complex relationships between structure and function in this region in health and disease (Eickhoff et al. 2005; Eickhoff, Heim, et al. 2006).

Anatomical Variability of Areas

We observed a strong interindividual anatomical variability of the superior parietal cytoarchitectonic areas in the present study. Previously, CV values for the whole parietal lobe volume (gray and white matter) between 0.09 and 0.13 were reported (Allen et al. 2002). Based on the fresh absolute volumes that we calculated for the SPC in our sample, including only gray matter, our values were about twice as high (female: 0.21; male: 0.25; area hIP3 excluded) and comparable to those of a previous study (Kennedy et al. 1998). This suggests that the volume variability in the SPC is stronger for the gray than for the white matter. Kennedy et al. (1998) also described regionally differential cortical volume variability in the SPC, namely lower variation of volumes in the PrC than in the SPL (CV: 0.13–0.35). This is in line with our finding of a trend toward higher volume variability for lateral areas compared with medial areas 5Ci and 7M (Fig. 12).

We demonstrated that a considerable number of cytoarchitectonic borders are not present in every brain (Table 2). Additionally, the locations of these borders are not reliably associated with macroanatomical landmarks (Scheperjans et al. 2007). We conclude that, although a basic constant pattern of areas exists in the SPC (see above; Figs. 6–10), the precise arrangement of areas and borders, however, is not identical in every brain, due to anatomical variations of areas within this pattern. This is in line with a recent study demonstrating a strong interindividual variability of the pattern of functionally identified areas in the SPC and IPS (Hagler et al. 2007). These findings argue against the assumption underlying nearly all historical cortical maps (Brodmann 1909, 1914; Vogt,1911; von Economo and Koskinas 1925; Gerhardt 1940; Sarkisov et al. 1955; Batsch 1956) and also their adaptations used frequently as anatomical reference for modern imaging experiments (Talairach and Tournoux 1988), that there is a constant pattern of areas and borders common to all individual human brains. This demonstrates the need for a probabilistic anatomical reference that accounts for this intersubject variability (Amunts and Zilles 2001; Zilles et al. 2002; Eickhoff et al. 2005; Eickhoff, Heim, et al. 2006).

Differences between Hemispheres and Genders

Stereotaxic Centers of Gravity

In our sample, the position of the centers of gravity for posterior subareas of BA 7 (areas 7P and 7M) was significantly more lateral in the right hemisphere. Putative methodological factors that may influence left–right differences were minimized. First, during fixation the brains were hanging on their basilar artery to avoid weight-induced shifts to one or the other

hemisphere and subsequent deformations induced by contact with the container (Amunts et al. 2000; Scheperjans et al. 2007). Second, for the analysis of interhemispheric differences, only a linear alignment of the postmortem brains to the reference brain was applied that transforms both hemispheres in the same manner (Amunts et al. 2000). Furthermore, in parallel with the interhemispheric difference observed for the center of area 7P, this area also showed interhemispheric asymmetries in terms of the location of its borders in relation to anatomical landmarks, as we reported in a previous study (Scheperjans et al. 2007). Therefore, this interhemispheric asymmetry in location likely reflects a topographical asymmetry of the living human brain with potential functional relevance and appears to be independent of gender.

Volume

A comparison of our data with previously published macrostructural investigations is not easy due to varying sample sizes, different measured parameters, and various techniques used for the definition of regions of interest. All these points may be responsible for conflicting results. One study reported that the volume of the whole parietal lobe (gray and white matter) was larger in males and showed a rightward asymmetry in females (Allen et al. 2002; $n_m + n_f = 23 + 23$). Reports about gray matter asymmetries are inconsistent. Asymmetries in terms of cortical thickness have been reported for the SPL (left > right) and PrC (right > left) with more pronounced differences in men (Luders et al. 2006; $n_m + n_f = 30 + 30$). A 2nd study measured higher volume of the SPC in males without asymmetries (Kennedy et al. 1998; $n_m + n_f = 10 + 10$). A 3rd publication reported no hemispheric asymmetries but a higher parietal gray matter concentration in females (Good et al. 2001b; $n_m + n_f = 265 + 200$), whereas another mentioned higher amounts of parietal gray matter in the left hemispheres of both genders (Watkins et al. 2001; $n_m + n_f = 81 + 61$). A more recent study reported that only in the left hemisphere the volume of parietal gray matter was larger in males and that only in females there was a rightward asymmetry (Allen et al. 2003; $n_m + n_f = 23 + 23$).

The abovementioned studies demonstrate that differential parietal macroanatomy between genders and hemispheres still is a matter of debate. Our volumetric methods have shown good sensitivity for detection of interhemispheric or gender-related differences in sample sizes comparable to that of the present study (Amunts et al. 2007). For example, it was recently demonstrated for the visual cortex that volume differences between genders do not necessarily involve a whole cortical lobe but can affect individual cytoarchitectonic areas specifically (Amunts et al. 2007). Such structural differences may be functionally relevant. However, they cannot be reliably detected when volumetric measurements are performed in regions of interest that are defined by macroscopical landmarks only, waiving microstructural information.

In the present study, we found no significant interhemispheric or gender-related volume differences for the areas of the SPC after adjustment for differences of total brain volume (Fig. 12). Also, no interhemispheric or gender differences of cytoarchitecture were detected in the study preceding this investigation (Scheperjans et al. 2007). When comparing our results with those of Amunts et al. (2007), it must be considered that gender differences of brain size are generally more pronounced in the frontal and occipital lobes than in the parietal region (Sowell et al. 2007). Our findings are in agreement with a recent study of cortical thickness in a large sample ($n_m + n_f = 90 + 86$) in which gender differences in the SPC were not significant and far less pronounced than in the inferior parietal cortex (Sowell et al. 2007). However, gender- and hemisphere-specific differences in brain activation patterns have been described for the SPC (see below) and may be associated with other anatomical asymmetries. For example, rightward asymmetry of superior parietal white matter pathways was recently demonstrated (Barrick et al. 2007).

Topographical Pattern of Areas

Significant interhemispheric differences for individual areas were detected concerning their stereotaxic location (7P, 7M) but not concerning their volume fractions. No interhemispheric differences were observed in terms of the probability of mutual borders between areas. However, in a previous study (Scheperjans et al. 2007), we demonstrated that the relative location of certain cytoarchitectonic areas/borders to macroanatomical landmarks shows interhemispheric differences. Taken together, these findings suggest that, within each subject, the relative positional pattern of areas and borders in the SPC was similar in both hemispheres, whereas within this pattern there were systematic spatial shifts between left and right hemispheres. These shifts were associated with differences mainly of the position but less of the volume fraction of areas.

Anatomical Variability

A previous study reported higher CV values for the whole parietal lobe volume for females and the right hemisphere (Allen et al. 2002), whereas a higher CV for the cortical volume of the SPL in females and no gender difference in the PrC were observed in another publication (Kennedy et al. 1998). To our knowledge, our study is the 1st to present volumetric data for the SPC that is not based on macroscopically defined regions of interest but on cytoarchitectonically defined areas. We found no significant interhemispheric or gender differences of volume variation after adjustment for differences of total brain volume (Fig. 12). However, there was a trend toward higher volume variability in males for several areas (5M, 5L, 7PC, 7A, hIP3). Additionally, hemisphere and gender had significant influence on the variability of the stereotaxic location of several areas (5M, 7PC, 7A, 7P), and interhemispheric differences of stereotaxic variation were gender specific in parts of BA 5 (Fig. 11). Thus, we demonstrated that the intersubject anatomical variations of different cytoarchitectonic areas underlie different gender- and hemisphere-specific influences. Therefore, differences in the selection of the regions of interest between volumetric studies may be an important factor for disagreements. A possible genetic background and functional correlates of these findings remain to be elucidated; however, our results may have implications for the design and interpretation of functional imaging studies (see below).

Implications for Functional Imaging Experiments

It is not completely understood what kind of structural correlates may underlie reported functional/behavioral differences between parietal areas (see above) and between hemispheres, genders, or individual subjects (see below). Nevertheless, it seems reasonable to assume that structural

differences are related to differential functional properties (see above; Scheperjans, Palomero-Gallagher, et al. 2005), and indeed, associations of parietal gray and white matter organization and performance in visuospatial tasks have been demonstrated recently (Meyer-Lindenberg et al. 2004; Eckert et al. 2005; Tuch et al. 2005; Wolbers et al. 2006). In previous imaging studies, many tasks involving reaching were associated with contra- or bilateral superior parietal activations (Culham et al. 2006; Filimon et al. 2007). Rightward lateralization has been described for attentional processes, movement planning, and visuomotor transformations (Barthélémy and Boulinguez 2002; Culham et al. 2006) and may be related to the structural asymmetries observed in the present study. However, with respect to visuospatial tasks, it is important to note that interhemispheric integration and functional connectivity of the SPC are context dependent (Stephan et al. 2007) and that therefore differential hemispheric involvement must not necessarily manifest itself as constant interhemispheric anatomical differences.

As demonstrated here and in our previous study (Scheperjans et al. 2007), there are strong and regionally differential intersubject anatomical variations of the cytoarchitectonic areas in the SPC (see above), and it is not possible to predict the precise location of these cytoarchitectonic areas and their borders on the basis of macroanatomical landmarks (Zilles et al. 2002; Uylings et al. 2005). When in functional imaging studies (e.g., functional magnetic resonance imaging) brain activations are analyzed, the individual data sets are spatially normalized to correct for macroanatomical intersubject variation before statistical analysis across subjects. The applied algorithms are usually based on the alignment of macroanatomical features and corresponding parts of the individual brains get superimposed. If, in such a study, a group of subjects performs a specific task, the same cytoarchitectonic area may get specifically activated in all subjects. If this microanatomical area would always be found at the same position in relation to macroanatomical landmarks, it could be expected that the voxels representing this area in the individual subjects are all superimposed at the same stereotaxic location after normalization, resulting in a significant activation in these voxels across subjects. However, if such a cytoarchitectonic area varied in size and location between subjects independently of macroanatomical landmarks, as demonstrated here for the areas of the SPC, the individual activations would not necessarily be superimposed after spatial normalization. This factor is not considered in the commonly used anatomical references (Talairach and Tournoux 1988) and has the potential to blur the activation in the group analysis for areas with high variability so that no significant activation would be detected. Consequently, the high anatomical variability of cytoarchitectonic areas in the SPC may have been a contributing factor in studies that showed a reduction of sensitivity in group analyses caused by differential parietal activation patterns between subjects performing the same task (e.g., motor skill acquisition; Schlaug et al. 1994).

Different intensities of these variations between areas (Fig. 12) may contribute to the observation that activations of some areas are detected in both single-subject and group analyses, whereas activations of other areas are obscured on the group level (Schlaug et al. 1994). Furthermore, the higher anatomical variability in left areas 7A and 7P (SPL), that is not found for area 7M (PrC), may result in a lower sensitivity for the detection of left-sided SPL activations and may have confounded previous imaging studies reporting that functional lateralization is less pronounced in the PrC, compared with the SPL (Cavanna and Trimble 2006).

It is well established that men on average perform better than women in visuospatial tasks like mental rotation (Voyer et al. 1995) or navigation (Astur et al. 1998). The relationship of this phenomenon to brain activation patterns in the SPC is under discussion. There is disagreement about the theory that differential activation patterns for men and women are not gender specific but for the most part explicable by differences in performance (Grön et al. 2000; Unterrainer et al. 2000, 2005; Jordan et al. 2002; Weiss et al. 2003; Boghi et al. 2006; Halari et al. 2006; Ohnishi et al. 2006; Gorbet and Sergio 2007). The here presented findings may be important for the design and interpretation of functional imaging studies analyzing such differences. For example, a recent study reported stronger bilateral activation at the junction of the PoCS and IPS in women compared with men during a mental rotation task independent of performance (Jordan et al. 2002). It is possible that in the group analysis of male subjects an anterior superior parietal activation of, for example, area 7PC, was weaker detected due to stronger anatomical variability in comparison with the female group. It has furthermore been suggested that 1 reason for the superior visuospatial performance in males is their stronger rightward functional lateralization in the parietal lobe (Gur et al. 2000), but this has been challenged by other authors (Dietrich et al. 2001; Halari et al. 2006). The stronger left-sided variability in men for parts of BA 5 could reduce the sensitivity for the detection of activations in the left hemisphere of male subjects and a similar effect may be relevant for righthemispheric activations in females. Such factors could bias analyses of gender-specific functional asymmetries and have so far not been considered in functional imaging studies.

The probabilistic maps of the SPC presented here constitute an objective anatomical reference and allow separate analyses for each cytoarchitectonic area in both hemispheres. They furthermore account for interindividual variability. By integrating them into functional imaging studies (Eickhoff et al. 2005; Eickhoff, Heim, et al. 2006), researchers can now investigate the complex structure–function relationships in this brain region more precisely and reliably.

Funding

Deutsche Forschungsgemeinschaft (KFO 112); a Human Brain Project/Neuroinformatics Research grant funded jointly by The National Institute of Biomedical Imaging and Bioengineering, The National Institute of Neurological Disorders and Stroke, and The National Institute of Mental Health; European Commission (QLG3-CT-2002-00746); Helmholtz Gemeinschaft.

Notes

Conflict of Interest: None declared.

Address correspondence to Filip Scheperjans, Institute of Medicine, Forschungszentrum Jülich GmbH, 52425 Jülich, Germany. Email: filip@gmx.net.

References

Allen JS, Damasio H, Grabowski TJ. 2002. Normal neuroanatomical variation in the human brain: an MRI-volumetric study. Am J Phys Anthropol. 118:341–358.

Allen JS, Damasio H, Grabowski TJ, Bruss J, Zhang W. 2003. Sexual dimorphism and asymmetries in the gray-white composition of the human cerebrum. Neuroimage. 18:880–894.
Allison T, McCarthy G, Luby M, Puce A, Spencer DD. 1996. Localization of functional regions of human mesial cortex by somatosensory evoked potential recording and by cortical stimulation. Electroencephalogr Clin Neurophysiol. 100:126–140.
Amunts K, Armstrong E, Malikovic A, Homke L, Mohlberg H, Schleicher A, Zilles K. 2007. Gender-specific left-right asymmetries in human visual cortex. J Neurosci. 27:1356–1364.
Amunts K, Kedo O, Kindler M, Pieperhoff P, Mohlberg H, Shah NJ, Habel U, Schneider F, Zilles K. 2005. Cytoarchitectonic mapping of the human amygdala, hippocampal region and entorhinal cortex: intersubject variability and probability maps. Anat Embryol (Berl). 210:343–352.
Amunts K, Malikovic A, Mohlberg H, Schormann T, Zilles K. 2000. Brodmann's areas 17 and 18 brought into stereotaxic space—where and how variable? Neuroimage. 11:66–84.
Amunts K, Schleicher A, Burgel U, Mohlberg H, Uylings HB, Zilles K. 1999. Broca's region revisited: cytoarchitecture and intersubject variability. J Comp Neurol. 412:319–341.
Amunts K, Zilles K. 2001. Advances in cytoarchitectonic mapping of the human cerebral cortex. Neuroimaging Clin N Am. 11:151–69, vii.
Astur RS, Ortiz ML, Sutherland RJ. 1998. A characterization of performance by men and women in a virtual Morris water task: a large and reliable sex difference. Behav Brain Res. 93:185–190.
Barrick TR, Lawes IN, Mackay CE, Clark CA. 2007. White matter pathway asymmetry underlies functional lateralization. Cereb Cortex. 17:591–598.
Barthélémy S, Boulinguez P. 2002. Manual asymmetries in the directional coding of reaching: further evidence for hemispatial effects and right hemisphere dominance for movement planning. Exp Brain Res. 147:305–312.
Batsch EG. 1956. Die myeloarchitektonische Untergliederung des Isocortex parietalis beim Menschen. J Hirnforsch. 2:225–258.
Battaglia-Mayer A, Caminiti R. 2002. Optic ataxia as a result of the breakdown of the global tuning fields of parietal neurones. Brain. 125:225–237.
Boghi A, Rasetti R, Avidano F, Manzone C, Orsi L, D'Agata F, Caroppo P, Bergui M, Rocca P, Pulvirenti L, et al. 2006. The effect of gender on planning: an fMRI study using the Tower of London task. Neuroimage. 33:999–1010.
Brodmann K. 1909. Vergleichende Lokalisationslehre der Großhirnrinde—in ihren Prinzipien dargestellt auf Grund des Zellenbaues. Leipzig (DE): Johann Ambrosius Barth.
Brodmann K. 1914. Physiologie des Gehirns. In: Bruns B, editor. Neue deutsche Chirurgie: die allgemeine Chirurgie der Gehirnkrankheiten. Vol. 11. Stuttgart (DE): Ferdinand Enke. p. 85–426.
Caminiti R, Ferraina S, Johnson PB. 1996. The sources of visual information to the primate frontal lobe: a novel role for the superior parietal lobule. Cereb Cortex. 6:319–328.
Caspers S, Geyer S, Schleicher A, Mohlberg H, Amunts K, Zilles K. 2006. The human inferior parietal cortex: cytoarchitectonic parcellation and interindividual variability. Neuroimage. 33:430–448.
Cavanna AE, Trimble MR. 2006. The precuneus: a review of its functional anatomy and behavioural correlates. Brain. 129:564–583.
Choi HJ, Zilles K, Mohlberg H, Schleicher A, Fink GR, Armstrong E, Amunts K. 2006. Cytoarchitectonic identification and probabilistic mapping of two distinct areas within the anterior ventral bank of the human intraparietal sulcus. J Comp Neurol. 495:53–69.
Culham JC, Cavina-Pratesi C, Singhal A. 2006. The role of parietal cortex in visuomotor control: what have we learned from neuroimaging? Neuropsychologia. 44:2668–2684.
Dietrich T, Krings T, Neulen J, Willmes K, Erberich S, Thron A, Sturm W. 2001. Effects of blood estrogen level on cortical activation patterns during cognitive activation as measured by functional MRI. Neuroimage. 13:425–432.
Eckert MA, Hu D, Eliez S, Bellugi U, Galaburda A, Korenberg J, Mills D, Reiss AL. 2005. Evidence for superior parietal impairment in Williams syndrome. Neurology. 64:152–153.
Eickhoff SB, Amunts K, Mohlberg H, Zilles K. 2006. The human parietal operculum. II. Stereotaxic maps and correlation with functional imaging results. Cereb Cortex. 16:268–279.
Eickhoff SB, Heim S, Zilles K, Amunts K. 2006. Testing anatomically specified hypotheses in functional imaging using cytoarchitectonic maps. Neuroimage. 32:570–582.
Eickhoff SB, Schleicher A, Scheperjans F, Palomero-Gallagher N, Zilles K. 2007. Analysis of neurotransmitter receptor distribution patterns in the cerebral cortex. Neuroimage. 34:1317–1330.
Eickhoff SB, Schleicher A, Zilles K, Amunts K. 2006. The human parietal operculum. I. Cytoarchitectonic mapping of subdivisions. Cereb Cortex. 16:254–267.
Eickhoff SB, Stephan KE, Mohlberg H, Grefkes C, Fink GR, Amunts K, Zilles K. 2005. A new SPM toolbox for combining probabilistic cytoarchitectonic maps and functional imaging data. Neuroimage. 25:1325–1335.
Evans AC, Marrett S, Neelin P, Collins L, Worsley K, Dai W, Milot S, Meyer E, Bub D. 1992. Anatomical mapping of functional activation in stereotactic coordinate space. Neuroimage. 1:43–53.
Fiehler K, Burke M, Engel A, Bien S, Rösler F. 2007. Kinesthetic Working Memory and Action Control within the Dorsal Stream. Cereb Cortex. doi:10.1093/cercor/bhm071.
Filimon F, Nelson JD, Hagler DJ, Sereno MI. 2007. Human cortical representations for reaching: mirror neurons for execution, observation, and imagery. Neuroimage. 37:1315–1328.
Gerhardt E. 1940. Die Cytoarchitektonik des Isocortex parietalis beim Menschen. J Psychol Neurol. 40:367–419.
Geyer S, Ledberg A, Schleicher A, Kinomura S, Schormann T, Burgel U, Klingberg T, Larsson J, Zilles K, Roland PE. 1996. Two different areas within the primary motor cortex of man. Nature. 382:805–807.
Geyer S, Schleicher A, Zilles K. 1999. Areas 3a, 3b, and 1 of human primary somatosensory cortex. Neuroimage. 10:63–83.
Good CD, Johnsrude IS, Ashburner J, Henson RNA, Friston KJ, Frackowiak RS. 2001a. A voxel-based morphometric study of ageing in 465 normal adult human brains. Neuroimage. 14:21–36.
Good CD, Johnsrude I, Ashburner J, Henson RN, Friston KJ, Frackowiak RS. 2001b. Cerebral asymmetry and the effects of sex and handedness on brain structure: a voxel-based morphometric analysis of 465 normal adult human brains. Neuroimage. 14:685–700.
Gorbet DJ, Sergio LE. 2007. Preliminary sex differences in human cortical BOLD fMRI activity during the preparation of increasingly complex visually guided movements. Eur J Neurosci. 25:1228–1239.
Grefkes C, Fink GR. 2005. The functional organization of the intraparietal sulcus in humans and monkeys. J Anat. 207:3–17.
Grefkes C, Geyer S, Schormann T, Roland P, Zilles K. 2001. Human somatosensory area 2: observer-independent cytoarchitectonic mapping, interindividual variability, and population map. Neuroimage. 14:617–631.
Grefkes C, Ritzl A, Zilles K, Fink GR. 2004. Human medial intraparietal cortex subserves visuomotor coordinate transformation. Neuroimage. 23:1494–1506.
Grön G, Wunderlich AP, Spitzer M, Tomczak R, Riepe MW. 2000. Brain activation during human navigation: gender-different neural networks as substrate of performance. Nat Neurosci. 3:404–408.
Gur RC, Alsop D, Glahn D, Petty R, Swanson CL, Maldjian JA, Turetsky BI, Detre JA, Gee J, Gur RE. 2000. An fMRI study of sex differences in regional activation to a verbal and a spatial task. Brain Lang. 74:157–170.
Hagler DJ Jr, Riecke L, Sereno MI. 2007. Parietal and superior frontal visuospatial maps activated by pointing and saccades. Neuroimage. 35:1562–1577.
Halari R, Sharma T, Hines M, Andrew C, Simmons A, Kumari V. 2006. Comparable fMRI activity with differential behavioural performance on mental rotation and overt verbal fluency tasks in healthy men and women. Exp Brain Res. 169:1–14.
Henn S, Schormann T, Engler K, Zilles K, Witsch K. 1997. Elastische Anpassung in der digitalen Bildverarbeitung auf mehreren Auflösungsstufen mit Hilfe von Mehrgitterverfahren. In: Paulus E, Wahl FM, editors. Mustererkennung. Berlin (DE): Springer. p. 392–399.

Hömke L. 2006. A multigrid method for anisotrophic PDE's in elastic image registration. Numer Linear Algebra Appl. 13:215–229.
Iacoboni M. 2006. Visuo-motor integration and control in the human posterior parietal cortex: evidence from TMS and fMRI. Neuropsychologia. 44:2691–2699.
Jones EG, Coulter JD, Hendry SH. 1978. Intracortical connectivity of architectonic fields in the somatic sensory, motor and parietal cortex of monkeys. J Comp Neurol. 181:291–347.
Jordan K, Wustenberg T, Heinze HJ, Peters M, Jancke L. 2002. Women and men exhibit different cortical activation patterns during mental rotation tasks. Neuropsychologia. 40:2397–2408.
Kennedy DN, Lange N, Makris N, Bates J, Meyer J, Caviness VS Jr. 1998. Gyri of the human neocortex: an MRI-based analysis of volume and variance. Cereb Cortex. 8:372–384.
Kretschmann HJ, Wingert F. 1971. Computeranwendungen bei Wachstumsproblemen in Biologie und Medizin. Berlin (DE): Springer.
Lacquaniti F, Guigon E, Bianchi L, Ferraina S, Caminiti R. 1995. Representing spatial information for limb movement: role of area 5 in the monkey. Cereb Cortex. 5:391–409.
Lewis JW, van Essen DC. 2000. Corticocortical connections of visual, sensorimotor, and multimodal processing areas in the parietal lobe of the macaque monkey. J Comp Neurol. 428:112–137.
Lim SH, Dinner DS, Pillay PK, Luders H, Morris HH, Klem G, Wyllie E, Awad IA. 1994. Functional anatomy of the human supplementary sensorimotor area: results of extraoperative electrical stimulation. Electroencephalogr Clin Neurophysiol. 91:179–193.
Luders E, Narr KL, Thompson PM, Rex DE, Jancke L, Toga AW. 2006. Hemispheric asymmetries in cortical thickness. Cereb Cortex. 16:1232–1238.
Macaluso E, Driver J, Frith CD. 2003. Multimodal spatial representations engaged in human parietal cortex during both saccadic and manual spatial orienting. Curr Biol. 13:990–999.
Malikovic A, Amunts K, Schleicher A, Mohlberg H, Eickhoff SB, Wilms M, Palomero-Gallagher N, Armstrong E, Zilles K. 2007. Cytoarchitectonic analysis of the human extrastriate cortex in the region of V5/MT+: a probabilistic, stereotaxic map of area hOc5. Cereb Cortex. 17:562–574.
Mangin JF, Riviere D, Cachia A, Duchesnay E, Cointepas Y, Papadopoulos-Orfanos D, Collins DL, Evans AC, Regis J. 2004. Object-based morphometry of the cerebral cortex. IEEE Trans Med Imaging. 23:968–982.
Marconi B, Genovesio A, Battaglia-Mayer A, Ferraina S, Squatrito S, Molinari M, Lacquaniti F, Caminiti R. 2001. Eye-hand coordination during reaching. I. Anatomical relationships between parietal and frontal cortex. Cereb Cortex. 11:513–527.
Matelli M, Govoni P, Galletti C, Kutz DF, Luppino G. 1998. Superior area 6 afferents from the superior parietal lobule in the macaque monkey. J Comp Neurol. 402:327–352.
Mazziotta J, Toga A, Evans A, Fox P, Lancaster J, Zilles K, Woods R, Paus T, Simpson G, Pike B, et al. 2001. A probabilistic atlas and reference system for the human brain: International Consortium for Brain Mapping (ICBM). Philos Trans R Soc Lond B Biol Sci. 356:1293–1322.
Meyer-Lindenberg A, Kohn P, Mervis CB, Kippenhan JS, Olsen RK, Morris CA, Berman KF. 2004. Neural basis of genetically determined visuospatial construction deficit in Williams syndrome. Neuron. 43:623–631.
Meyer-Lindenberg A, Mervis CB, Berman KF. 2006. Neural mechanisms in Williams syndrome: a unique window to genetic influences on cognition and behaviour. Nat Rev Neurosci. 7:380–393.
Molenberghs P, Mesulam MM, Peeters R, Vandenberghe RR. 2007. Remapping attentional priorities: differential contribution of superior parietal lobule and intraparietal sulcus. Cereb Cortex. 17:2703–2712.
Moore TL, Schettler SP, Killiany RJ, Herndon JG, Luebke JI, Moss MB, Rosene DL. 2005. Cognitive impairment in aged rhesus monkeys associated with monoamine receptors in the prefrontal cortex. Behav Brain Res. 160:208–221.
Morecraft RJ, Cipolloni PB, Stilwell-Morecraft KS, Gedney MT, Pandya DN. 2004. Cytoarchitecture and cortical connections of the posterior cingulate and adjacent somatosensory fields in the rhesus monkey. J Comp Neurol. 469:37–69.
Morosan P, Rademacher J, Schleicher A, Amunts K, Schormann T, Zilles K. 2001. Human primary auditory cortex: cytoarchitectonic subdivisions and mapping into a spatial reference system. Neuroimage. 13:684–701.
Mountcastle VB, Lynch JC, Georgopoulos A, Sakata H, Acuna C. 1975. Posterior parietal association cortex of the monkey: command functions for operations within extrapersonal space. J Neurophysiol. 38:871–908.
Northoff G, Heinzel A, de GM, Bermpohl F, Dobrowolny H, Panksepp J. 2006. Self-referential processing in our brain—a meta-analysis of imaging studies on the self. Neuroimage. 31:440–457.
Ohnishi T, Matsuda H, Hirakata M, Ugawa Y. 2006. Navigation ability dependent neural activation in the human brain: an fMRI study. Neurosci Res. 55:361–369.
Orban GA, Claeys K, Nelissen K, Smans R, Sunaert S, Todd JT, Wardak C, Durand JB, Vanduffel W. 2006. Mapping the parietal cortex of human and non-human primates. Neuropsychologia. 44:2647–2667.
Pandya DN, Seltzer B. 1982. Intrinsic connections and architectonics of posterior parietal cortex in the rhesus monkey. J Comp Neurol. 204:196–210.
Raichle ME, MacLeod AM, Snyder AZ, Powers WJ, Gusnard DA, Shulman GL. 2001. A default mode of brain function. Proc Natl Acad Sci USA. 98:676–682.
Raz N, Gunning FM, Head D, Dupuis JH, McQuain J, Briggs SD, Loken WJ, Thornton AE, Acker JD. 1997. Selective aging of the human cerebral cortex observed in vivo: differential vulnerability of the prefrontal gray matter. Cereb Cortex. 7:268–282.
Rottschy C, Eickhoff SB, Schleicher A, Mohlberg H, Kujovic M, Zilles K, Amunts K. 2007. Ventral visual cortex in humans: cytoarchitectonic mapping of two extrastriate areas. Hum Brain Mapp. 28:1045–1059.
Rushworth MF, Behrens TE, Johansen-Berg H. 2006. Connection patterns distinguish 3 regions of human parietal cortex. Cereb Cortex. 16:1418–1430.
Sakakibara R, Fowler CJ, Hattori T. 1999. Voiding and MRI analysis of the brain. Int Urogynecol J Pelvic Floor Dysfunct. 10:192–199.
Sarkisov SA, Filimonoff IN, Kononowa EP, Preobraschenskaja IS, Kukuew LA. 1955. Atlas of the cytoarchitectonics of the human cerebral cortex. Moscow (RU): Medgiz.
Scheperjans F, Grefkes C, Palomero-Gallagher N, Schleicher A, Zilles K. 2005. Subdivisions of human parietal area 5 revealed by quantitative receptor autoradiography: a parietal region between motor, somatosensory, and cingulate cortical areas. Neuroimage. 25:975–992.
Scheperjans F, Hermann K, Eickhoff SB, Amunts K, Schleicher A, Zilles K. 2007. Observer-independent cytoarchitectonic mapping of the human superior parietal cortex. Cereb Cortex. doi:10.1093/cercor/bhm116.
Scheperjans F, Palomero-Gallagher N, Grefkes C, Schleicher A, Zilles K. 2005. Transmitter receptors reveal segregation of cortical areas in the human superior parietal cortex: relations to visual and somatosensory regions. Neuroimage. 28:362–379.
Schlaug G, Knorr U, Seitz R. 1994. Inter-subject variability of cerebral activations in acquiring a motor skill: a study with positron emission tomography. Exp Brain Res. 98:523–534.
Schleicher A, Amunts K, Geyer S, Kowalski T, Schormann T, Palomero-Gallagher N, Zilles K. 2000. A stereological approach to human cortical architecture: identification and delineation of cortical areas. J Chem Neuroanat. 20:31–47.
Schleicher A, Amunts K, Geyer S, Morosan P, Zilles K. 1999. Observer-independent method for microstructural parcellation of cerebral cortex: a quantitative approach to cytoarchitectonics. Neuroimage. 9:165–177.
Schleicher A, Palomero-Gallagher N, Morosan P, Eickhoff SB, Kowalski T, de VK, Amunts K, Zilles K. 2005. Quantitative architectural analysis: a new approach to cortical mapping. Anat Embryol (Berl). 210:373–386.
Sereno MI, Huang RS. 2006. A human parietal face area contains aligned head-centered visual and tactile maps. Nat Neurosci. 9:1337–1343.

Shima K, Aya K, Mushiake H, Inase M, Aizawa H, Tanji J. 1991. Two movement-related foci in the primate cingulate cortex observed in signal-triggered and self-paced forelimb movements. J Neurophysiol. 65:188–202.
Simon O, Kherif F, Flandin G, Poline JB, Riviere D, Mangin JF, Le BD, Dehaene S. 2004. Automatized clustering and functional geometry of human parietofrontal networks for language, space, and number. Neuroimage. 23:1192–1202.
Sowell ER, Peterson BS, Kan E, Woods RP, Yoshii J, Bansal R, Xu D, Zhu H, Thompson PM, Toga AW. 2007. Sex differences in cortical thickness mapped in 176 healthy individuals between 7 and 87 years of age. Cereb Cortex. 17:1550–1560.
Stephan KE, Marshall JC, Penny WD, Friston KJ, Fink GR. 2007. Interhemispheric integration of visual processing during task-driven lateralization. J Neurosci. 27:3512–3522.
Stoeckel MC, Weder B, Binkofski F, Choi HJ, Amunts K, Pieperhoff P, Shah NJ, Seitz RJ. 2004. Left and right superior parietal lobule in tactile object discrimination. Eur J Neurosci. 19:1067–1072.
Talairach J, Tournoux P. 1988. Co-planar stereotaxic atlas of the human brain. Stuttgart (DE): Thieme.
Tuch DS, Salat DH, Wisco JJ, Zaleta AK, Hevelone ND, Rosas HD. 2005. Choice reaction time performance correlates with diffusion anisotropy in white matter pathways supporting visuospatial attention. Proc Natl Acad Sci USA. 102:12212–12217.
Unterrainer J, Wranek U, Staffen W, Gruber T, Ladurner G. 2000. Lateralized cognitive visuospatial processing: is it primarily gender-related or due to quality of performance? A HMPAO-SPECT study. Neuropsychobiology. 41:95–101.
Unterrainer JM, Ruff CC, Rahm B, Kaller CP, Spreer J, Schwarzwald R, Halsband U. 2005. The influence of sex differences and individual task performance on brain activation during planning. Neuroimage. 24:586–590.
Uylings HB, Rajkowska G, Sanz-Arigita E, Amunts K, Zilles K. 2005. Consequences of large interindividual variability for human brain atlases: converging macroscopical imaging and microscopical neuroanatomy. Anat Embryol (Berl). 210:423–431.
Uylings HB, van Eden CG, Hofman MA. 1986. Morphometry of size/volume variables and comparison of their bivariate relations in the nervous system under different conditions. J Neurosci Methods. 18:19–37.
van Essen DC. 2004. Towards a quantitative, probabilistic neuroanatomy of cerebral cortex. Cortex. 40:211–212.
Vogt O. 1911. Die Myeloarchitektonik des Isocortex parietalis. J Psychol Neurol. 18:379–390.
von Economo C, Koskinas GN. 1925. Die Cytoarchitektonik der Hirnrinde des erwachsenen Menschen. Wien (AT): Julius Springer.
Voyer D, Voyer S, Bryden MP. 1995. Magnitude of sex differences in spatial abilities: a meta-analysis and consideration of critical variables. Psychol Bull. 117:250–270.
Watkins KE, Paus T, Lerch JP, Zijdenbos A, Collins DL, Neelin P, Taylor J, Worsley KJ, Evans AC. 2001. Structural asymmetries in the human brain: a voxel-based statistical analysis of 142 MRI scans. Cereb Cortex. 11:868–877.
Weiss E, Siedentopf CM, Hofer A, Deisenhammer EA, Hoptman MJ, Kremser C, Golaszewski S, Felber S, Fleischhacker WW, Delazer M. 2003. Sex differences in brain activation pattern during a visuospatial cognitive task: a functional magnetic resonance imaging study in healthy volunteers. Neurosci Lett. 344:169–172.
Wenderoth N, Toni I, Bedeleem S, Debaere F, Swinnen SP. 2006. Information processing in human parieto-frontal circuits during goal-directed bimanual movements. Neuroimage. 31:264–278.
Wolbers T, Schoell ED, Buchel C. 2006. The predictive value of white matter organization in posterior parietal cortex for spatial visualization ability. Neuroimage. 32:1450–1455.
Zilles K, Eickhoff S, Palomero-Gallagher N. 2003. The human parietal cortex: a novel approach to its architectonic mapping. Adv Neurol. 93:1–21.
Zilles K, Schleicher A, Palomero-Gallagher N, Amunts K. 2002. Quantitative analysis of cyto- and receptorarchitecture of the human brain. In: Toga A, Mazziotta J, editors. Brain mapping: the methods. 2nd ed. San Diego (CA): Academic Press. p. 573–602.